## ABSTRACT

KUNDU, PRITHWISH. Gas Turbine Combustion Chamber Design for Viscous Fuels.
(Under the direction of Dr. William L Roberts.)

Combustion of low grade fuels has always posed a challenge in all combustion applications. High viscosity and enthalpy of vaporization make fuels like glycerin very difficult to burn. Crude glycerin is by product of bio diesel production. Owing to the high volume of bio diesel production, burning the huge amounts of glycerin cleanly is proving to be a good alternative for its disposal. However it is difficult to achieve a stable flame with glycerin as a fuel. Some solutions from previous research have been implemented into this current work to burn glycerin in a gas turbine combustion chamber. A cyclone combustor type of design was developed. However this cyclone burner was very different from the other tangential feed burners. A new design for introducing swirl was implemented to burn glycerin successfully. In this process a CFD model was developed that could give insight into the flow dynamics of the burner and be used as a tool.

Gas Turbine Combustion Chamber Design for Viscous Fuels

by
Prithwish Kundu

A thesis submitted to the Graduate Faculty of
North Carolina State University
in partial fulfillment of the
requirements for the degree of
Master of Science

Mechanical Engineering

Raleigh, North Carolina

2012

APPROVED BY:

| | |
|---|---|
| _____ | _____ |
| Dr.William L Roberts<br>Committee Co- Chair | Dr.Alexei Saveliev<br>Committee Co-Chair |

_____
Dr.Tiegang Fang
Committee Member

# DEDICATION

Dedicated to my parents

## ACKNOWLEDGMENTS

I would like to thank the following people for their help and support.
Dr. William Roberts
Dr. Alexei Saveliev
Dr. Tiegang Fang
Joseph Scroggins
Brian McCain
Myles Bohon
Joel Lisanti
Fei
John Sayers
Robbie Little
Myrrha Anderson
Avineet Ponde
Guriqbal Singh
Richa Sinha
Sriram Pakkam

## TABLE OF CONTENTS

## LIST OF FIGURES

# Chapter 1

# Introduction

## 1.1 Why burn glycerin?

In recent years the production of bio diesel has grown substantially all over the world. In biodiesel production glycerin is a major byproduct, almost 10% by volume depending on the feedstock used to produce biodiesel. This is a very high amount of glycerin considering the fact that the total production of biodiesel was 20,000 million liters [1] for the year 2011 and is expected to grow even more in the coming years. The glycerin produced as a by- product of biodiesel production contains a lot of impurities and market for crude glycerin is saturated. The impurities mainly include salts and free fatty acids. This crude glycerin has to be purified to for the pharmaceutical or food industry. These impurities can be removed by nanofilteration, ion exchange and evaporation to remove water. These processes are expensive and time consuming. Thus crude glycerin is a cost and environmental liability for the biodiesel companies. Thus the huge amount of glycerin produced by biodiesel plants is a major issue. Discharging it into water bodies or land has harmful effects on the flora and fauna of the ecosystem. Also this would be against most of the environmental regulations. However pure glycerin has a low heating value of 16MJ/kg. Crude glycerin has a heating value of 12 to 26 MJ/kg depending on the sample [5] used. This results in a possibility of using glycerin as a fuel. The idea of using crude glycerin for direct combustion or

gasification and syngas production has been the subject of many studies [1-4]. Even though the heating value of glycerin is lower than the heating values of conventional fuels, it is abundantly available and the costs are also very low. Moreover if it can be burned cleanly then it would be the best way to dispose of the huge amounts of glycerin that are being produced by the biodiesel companies.

## 1.2 Difficulties in burning glycerin

It is found to be very difficult to burn glycerin. Glycerin has very high viscosity as compared to conventional fuels (1.412 Pa s) at room temperature. This is a major drawback in using glycerin as a fuel. Also it is difficult to vaporize glycerin due to its high latent heat. The ability of liquid fuels to vaporize quickly is very important as combustion would occur in gas phase. We would want to get into that phase as quickly as possible. Glycerin has high auto-ignition temperature of 370 °C. If glycerin decomposes it forms acrolein ($C_3H_4O$) which is poisonous and causes respiratory problems. The high viscosity of the fuel causes a lot of problems in spraying the fuel. The spray patterns and droplet formation also get severely affected due to high viscosity. For efficient combustion we would like to have a spray with very small droplets so that the fuel has a faster rate of evaporation. High viscosity hinders the process of the spray particle breakup. Another major issue with the combustion of glycerin is that we do not have a kinetic model available that could model the combustion mechanism of glycerin. This is also an added disadvantage as we cannot use reactive flow model already developed to design or predict the performance of our burner. The current work tries to find a solution to all these problems which are posed for the combustion of glycerin.

## 1.3 Some solutions for burning glycerin

Previous work by author [2] has shown that it is possible to burn glycerin with a stable flame. This can be done using a high swirl burner and hot radiating walls. This system needs to be preheated first using a conventional fuel like jet-A. If we can have hot radiating walls then these would enhance the droplet evaporation due to the radiation coming from the walls. Ceramics were found to be ideal for this situation. Also it was noted that the viscosity of glycerin decreases rapidly as it is heated. Thus if we can preheat the fuel then we can overcome some of the problems we face due to high viscosity of the fuel. This would make pumping and atomization of the fuel much easier.

## 1.4 Advantage of burning glycerin in a gas turbine

There are a number of ways in which we can produce work from a heat source which includes implementing a Rankine or a Brayton cycle.

To produce the maximum amount of work from any heat source we know that we would like to have a heat source at a temperature as high as possible and the heat sink temperature has to be as low as possible. Steam powered Rankine cycles have a limit on the temperature at which we are adding heat. In most power plants the working fluid is water which is incompressible when liquid and hence cannot be compressed to higher temperature before heat is being added. Brayton cycle powered gas turbines have a limiting factor when they are rejecting heat to the sink. Gas turbines generally have very high exhaust temperatures because they cannot expand the gases below the atmospheric pressures. However if both of these cycles are combined into a combined cycle cogeneration unit with the gas turbine

running on glycerin and then the exhaust gases used to run a Rankine cycle we will have much higher efficiencies. It has been shown that co generative power plants have much higher efficiencies than stand alone gas turbines or steam power plants. This can also be proved theoretically from the basic equations of thermodynamics as follows.

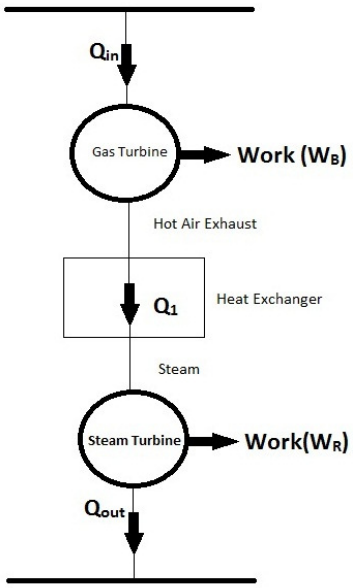


**Figure 1.1: Schematic of combined Rankine and Brayton cycle.**

The overall efficiency of the combined cycle can be derived as follows. We denote the heat received by the gas turbine as $Q_{in}$ and the heat rejected to the atmosphere as $Q_{out}$. The heat out of the gas turbine is denoted as $Q_1$. The hot exhaust gases from the gas turbine pass through a heat exchanger where they are used as the heat source for the two-phase Rankine cycle, so that $Q_1$ is also the heat input to the steam cycle. The overall combined cycle efficiency is

$$\eta_{\mathrm{CC}} = \frac{W}{Q_{\mathrm{in}}} = \frac{W_B + W_R}{Q_{\mathrm{in}}},$$

where the subscripts refer to combined cycle (CC), Brayton cycle (B) and Rankine cycle (R).

From the first law, the overall efficiency can be expressed in terms of the heat inputs and heat rejections of the two cycles as (using the quantity $|Q_1|$ to denote the magnitude of the heat transferred):

$$\eta_{\mathrm{CC}} = \frac{Q_{\mathrm{in}} - |Q_1| + (|Q_1| - Q_{\mathrm{out}})}{Q_{\mathrm{in}}} = \left[1 - \frac{|Q_1|}{Q_{\mathrm{in}}}\right] + \left[1 - \frac{Q_{\mathrm{out}}}{|Q_1|}\right]\left(\frac{|Q_1|}{Q_{\mathrm{in}}}\right).$$

The first square bracket term on the right hand side is the Brayton cycle efficiency, $\eta_B$ , the second is the Rankine cycle efficiency, $\eta_R$, and the term in parentheses is $(1- \eta_B)$ . The combined cycle efficiency can thus be written as

$$\eta_{CC} = \eta_B + \eta_R - \eta_B\, \eta_R$$

Now say we have a Brayton Cycle that has an efficiency of 30% and a Rankine cycle that has an efficiency of 30% then the overall efficiency of the combined cycle will be 51%. Thus we can achieve much higher efficiencies using a combined cycle. Thus if we want to burn glycerin on a large scale to produce work, namely electricity, then burning glycerin in a gas turbine would give us the option of implementing a combined cycle.

## 1.5 Additional challenges in burning glycerin in a gas turbine

The idea of burning glycerin in a gas turbine introduces even more complexities to an already complex problem. Gas turbine combustion always occurs at higher pressures and at much higher velocities. The conditions are more adverse for getting a stable flame. In a Rankine cycle we can burn fuel externally at atmospheric pressures to heat the working fluid. In the case of a Brayton cycle the fuel has to be injected into the working fluid, mix with the oxidizer at the molecular level, react and form saturated combustion products to add enthalpy to the fluid. The combustion products would be directly in contact with the turbine blades. This would mean that we need to be more careful with what our combustion products are and also the final temperatures of the combustion chamber exhaust gases. The exhaust temperatures should be well within the material constraints imposed by the turbine blades. Particulate matter present in the combustion products could be a major cause of concern. Earlier it was pointed out that hot radiating walls are a prerequisite for glycerin combustion. To achieve this we cannot use metal liners as they cannot withstand temperatures above 1300 K. Ceramics are better suited for this job and was also pointed out in previous work by Bohon et al. [2] . However drilling holes in ceramics is a complex process. This is a major cause of concern considering the fact that gas turbine combustion chambers require perforated liners for dilution holes. Also hot walls/regions are responsible for NOx formation. All these points make it a very challenging ask to burn glycerin in a gas turbine.

## 1.6 Thesis objectives

We now want to use glycerin as a fuel and burn it in a gas turbine for all the reasons discussed in the above sections. This can be achieved easily if we can modify only the combustion chamber of an existing gas turbine and retro fit it with our new design. This will give us the ability to work with existing gas turbines. The combustion chamber of the gas turbine is one of the most critical parts of the engine. This thesis aims to model and develop a combustion chamber that would pre heat on jet fuel and then switch over to glycerin. To predict the design performance of the combustion chamber we develop a CFD model using commercially available code CFX. This work aims at developing a CFD model especially for gas turbine combustion chambers with all provisions for modeling the complex combustion reactions and species transport in a reactive flow. The CFD model would be helpful in locating the swirl zones and to figure out the flow patterns that develop. The model will also help to predict emissions like NOx, CO and HCs. We would also want our CFD model to tell us best possible design for our combustion chamber. Finally we would want to refit an existing gas turbine's combustion chamber with our new design that would burn glycerin and produce power.

# Chapter 2

## Experimental Set Up

The previous research of Bohon et al. [2] utilized a high swirl stabilized turbulent flame with air atomizing nozzle, refractory lined walls for thermal feedback and recirculation zones. It was shown that the thermal feedback from the refractory lined walls was very important for quick evaporation of the liquid fuel droplets. Moreover it was necessary that the combustion chamber was preheated to a high enough temperature using a conventional fuel and then switching over to glycerin. These conclusions from previous research were used to develop the new combustion chamber. The current experimental setup was designed to combine the knowledge gained from previous research and the existing geometry of a GTCP 85-397 gas turbine, selected for its low pressure ratio and availability as a surplus engine. The apparatus as designed to be modular so that changes could be made easily to test for different geometries and configurations. Also the GTCP 85-397 had some added advantages. These gas turbines featured a single can combustor geometry that was easily accessible. This could be removed easily and modifications could be made easily and fitted with the retrofit combustion chamber. Before the newly designed combustion chamber was to be fitted to the gas turbine it was necessary to test it seperately. The following apparatus was designed for creating a test bed for the combustion chamber. There are three main components of the experimental set up: compressed air supply, the combustion chamber and the fuel delivery

system. The experimental setup is such that it allows us to test combustion chamber at atmospheric as well as pressurized conditions.

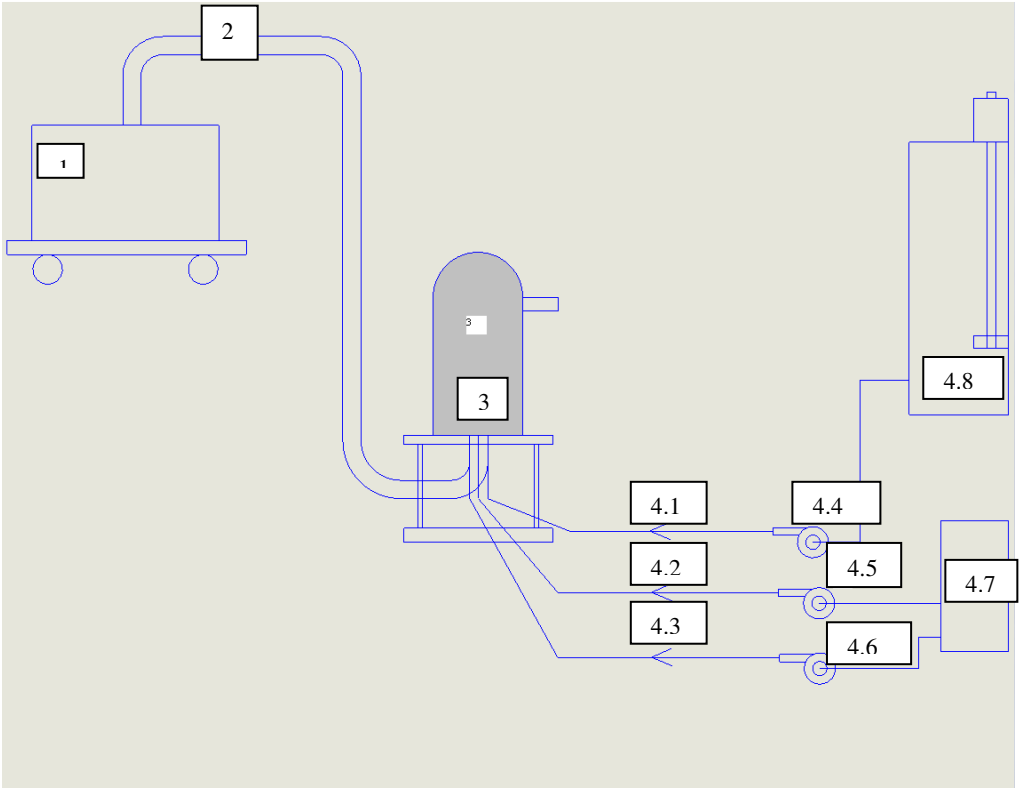


**Figure 2.1: Experimental setup schematic:**
**1-GTC85-90**
**2-Bleed air hose**
**3- Test stand and combustion chamber**
**4.1- Glycerin supply line**
**4.2- Jet-A supply line for pilot**
**4.3- Jet-A fuel supply line for main nozzle**
**4.4-Pump for glycerin**
**4.5- Pump for Jet-A pilot nozzle**
**4.6- Pump for Jet-A main nozzle.**
**4.7- Jet-A fuel tank**
**4.8- Heated glycerin tank**

## 2.1 Compressed air supply to combustion chamber

Gas turbines generally have very high mass flow rates. In order to simulate this we cannot use a compressed gas tank with reciprocating compressors as the tank would not be capable of providing the required mass flow rates for a long period of time. Also such sources of compressed air will not have the required high temperatures. Rotary compressors like axial flow and centrifugal compressors have the ability to deliver such mass flow rates at higher pressures and temperatures. A GTC85-90 “bleed air” gas turbine was used for this purpose. The turbine system selected was a Dash-60 gas turbine generator set. The Dash-60 gen-set was selected for a variety of reasons. First, the Dash-60 gen-set is powered by a Garrett AiResearch GTCP85-397 gas turbine system. The GTCP85-397 gas turbine is ideal because it operates with a low pressure ratio, approximately 3.5. While the low pressure ratio results in an inefficient system when compared to modern gas turbine systems, the low performance allows for safe modification and larger margin for error. The GTCP85-397 is readily available as a government surplus system. Additionally, the Dash-60 system has an electrical power generator attached to the turbine, as well as a control interface to toggle the power load. The generator is capable of producing 75 kVA, or 60 kW, of 120 V AC power at 400 Hz. Finally, other GTXX85 series turbines, which generally use similar components and have similar performance levels, are also readily available. To that end, a GTC85-90 “bleed air” gas turbine was acquired to allow us to develop an experimental combustion system that could replicate gas turbine conditions at the combustor inlet. The GTC85-90 gas turbine is designed to produce high enthalpy air flow and has a pressure ratio of 3.5 like the GTCP85-

397 turbine. The bleed air from the GTC85-90 thus exactly matches the combustor inlet temperature and pressure for the GTCP85-397 turbine, albeit at lower air flow rates. Its bleed air port can deliver 120 pounds per minute of air at 200C and 375 kPa. Typically these are ground power units (GPUs) and are used to start up bigger gas turbines. They are also used as auxiliary power units which are a key component in every modern aircraft. The high pressure air form the bleed port of these machines are typically used to start the main engines, hydraulic power source during engine failures and also to generate electrical power when the aircraft is waiting on the tarmac with its main engine switched off. We use this pressurized bleed air as the inlet air for our combustion chamber. This bleed air from the GTC85-90 is extracted from the bleed port through a hose which is 8.5 inches in diameter. This connects to the combustion chamber. A gate valve is fixed downstream of the bleed air port to control the mass flow rate of air. The combustion chamber exit is open to the atmosphere. Thus this type of set up would allow us to test combustion at atmospheric pressures. In this set up the entire pressure drop occurs across the gate valve and the pressure in the combustion chamber would be atmospheric. In order to test the combustion chamber under pressurized conditions a gate valve is placed at the exhaust port of the combustion chamber. When this restrictor is fully open then the pressure inside the combustion chamber is atmospheric. As we decrease the area of the restriction the pressure inside the combustion chamber increases. In this case the pressure drop occurs across the restriction of the second gate valve. A pressure gauge mounted on the combustion chamber indicates the pressure inside the combustion chamber.

**Figure 2.2: Dash-60 genset**

**Figure 2.3:GTC85-90 bleed air turbine**

## 2.2 Mass flow rate calibration:

Knowing the mass flow rate of air coming out from the bleed air port is very important. Knowing the mass flow rate is important to set the correct equivalence ratio. The velocities were measured at different locations of the hose cross section for given number of turns of the gate valve. The following diagram and table illustrates the positions where the velocities were measured. The velocities were measured for different values of r and ϴ along the hose cross section as shown in figure 2.4.

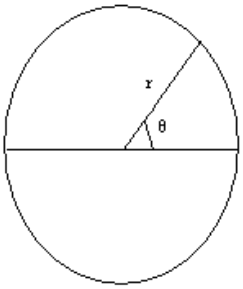


**Figure 2.4: Cross-section of bleed air hose.**

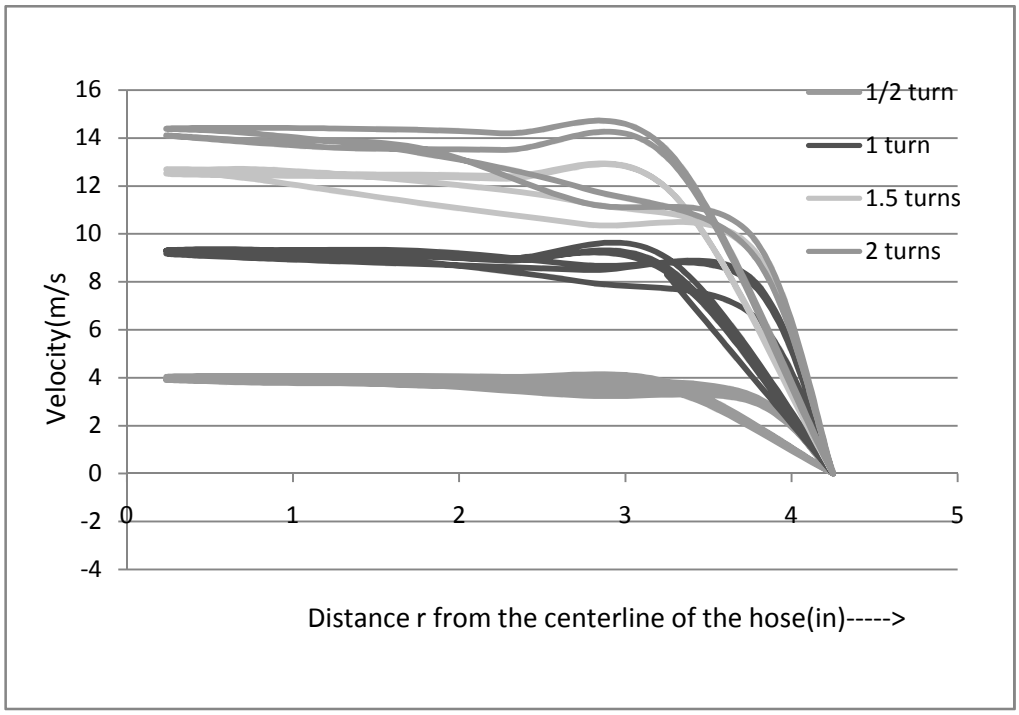


**Figure 2.5: Calibration of gate valve**

## 2.3 Fuel delivery system

The fuel delivery system is palette-mounted and capable of supplying fuel to the main Jet-A nozzle, the glycerin nozzle, and the pilot Jet-A nozzle. Each fuel line utilizes a Haldex pump, each capable of delivering up to 1.73 liters/min. Each pump is powered by an AC motor and controlled with a frequency controller. Dayton frequency controllers are used for the pilot Jet-A fuel and the glycerin pumps and a Telemecanique frequency controller are used for the main Jet-A system. The fuel lines primarily consist of 3/8" stainless steel tubing with Swagelok compression fittings, NPT fittings, and adapters. Both main fuel lines have valved

fuel delivery and fuel recirculation lines that allow the pump to run continuously while injecting neither, one, or both of the fuels. Both the main Jet-A line and pilot line have an in-line Hydac diesel filter. The glycerin fuel line has several filters and strainers, including a Marin Mfg. high-pressure filter after the outlet of the pump and a fine wire mesh on the intake. The fuel delivery palette houses the glycerin supply barrel. This barrel has been fitted with an in-barrel heater, capable of delivering 4500 W of power, as well as a 246 W motor with a stirring rod. The barrel has temperature monitoring points that help prevent scalding of the glycerin. Each fuel injection line has a quick disconnect fitting that allows for easy connection to the burner system. A control box houses switches that power both the main Jet-A pump system and the glycerin pump system. The box is fitted with potentiometers that serve to increase and decrease the frequency output by the frequency drive, and thus dictate the motor speed and fuel output. The control box also has a switch to turn on the igniter within the combustion chamber as well as a "*killswitch*" that turns off the entire system in case of an emergency. Figures 2.6 and 2.7 show the pumps, motors, lines, and control box. The fuel injection was calibrated by measuring the fuel mass sprayed through the nozzle over a period of time, typically 30 seconds to a minute, depending on the flow rate.

**Figure 2.6: Fuel cart with glycerin barrel**


**Figure 2.7: Control Box**

## 2.4 Test Stand

The experimental test stand was designed to allow us to study the combustion characteristics of our burner designs (figure 2.8). The stand was designed with uni-strut to support the weight of the combustion system. The test stand is wheeled so it can be easily moved from storage into position for experimentation. The burner plates described in later sections were mounted to the stand. Mounted below the burner plate is an 8 inch nominal diameter schedule 40 pipe 90° elbow. This pipe elbow was fitted with a flange with a specially designed fitting to attach to the bleed air hose from the GTC85-90 bleed air turbine. A gate valve mounted between the elbow and adapter allow us to control the total air flow rate from the bleed air turbine. The test stand also served at the base for the high pressure combustion tests.

**Figure 2.8: Test stand**

# Chapter 3

## CFD modeling of gas turbine combustion chamber

There are a number of factors and design parameters that influence the performance of a gas turbine combustion chamber. The reactive flow inside the chamber is very highly sensitive to design parameters and the operating conditions. It has been observed that these parameters also influence the emission levels. Thus it becomes very important to have an approximate idea as to how the flow field would look for a given design. However in order to test the effect of all these parameters it would involve a lot of experimental work and setup cost. In order to reduce this and to get an idea as to how our design is performing a CFD model would be helpful for the design process. It would also significantly reduce the number of experimental test cases. Thus it was decided to model the flow inside the combustion chamber. The following sequential process was adopted to model the flow inside the combustion chamber.

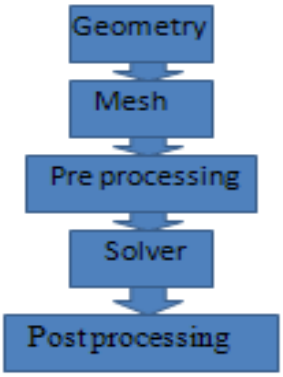


**Figure 3.1: CFD workflow**

## 3.1 Geometry

Creating the solid model for the components to be modeled is the first step. This was done using SolidWorks. Then it was imported in to Ansys DesignModeler.

**Figure 3.2: The swirler plate (left) and its solid model (right)**

In order to set up the CFD model initially the combustion chamber of the dash-60 genset was modeled. This would also give us some insight into the flow field of the combustor can which was to be replaced with the new retrofit which could also burn glycerin. The **figure 3.2** shows the solid model created using SolidWorks. However for a CFD analysis we need to model the fluid domain. Most of the modern meshing software uses the solid part of the geometry to create the mesh. The meshed region would be the fluid domain. Thus we need to inverse model the objects i.e. model the fluid domains as solid and the solid domains as hollow in our model. This was done by importing the solid geometries into Ansys DesignModeler and then inverting the model using "subtract body" commands.

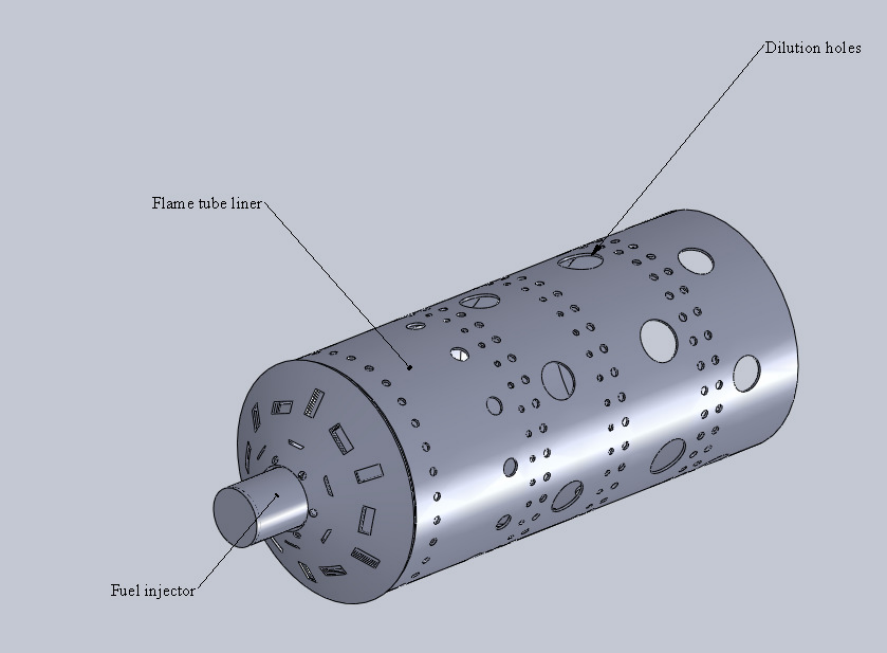


**Figure 3.3: Solid model of dash 60 combustor can**

## 3.2 Mesh

CFX Mesh is a mesh generator used to generate high quality 3-D meshes for CFD simulations. It creates tetrahedra, pyramids and prisms in 3D meshing mode. A number of methods are also available to control the surface and volume mesh parameters. Using these methods we can selectively make the mesh finer in some regions. Generally these are the regions where we expect maximum gradients in our fluid flow. Moreover the grids should also be fine enough to resolve the geometry accurately. We cannot have the smallest grid size throughout the whole geometry as that would increase the computational time significantly. Thus we would like to have a finer mesh in regions where the geometry is complex and also where we expect higher gradients in the flow field variables. These were done using the surface and volume mesh control techniques in CFX Mesh. Some CFD simulations can make effective use of periodic pair boundary conditions, which force the flow leaving at one face to re-enter at that face's equivalent in the periodic mapping. Periodic boundary conditions can significantly reduce our computational domain. If a model is axis-symmetric then instead of meshing and solving the entire 3D model we can simply cut out a wedge from the solid part and use periodic boundary conditions.

The ANSYS CFX Solver is capable of making more accurate calculations on this type of boundary condition if the mesh on each face in the periodic boundary is identical to the mesh on the equivalent face in the periodic mapping. The use of Periodicity allows generating identical meshes for faces that will later be specified as part of a periodic boundary condition in the simulation set-up. This is achieved by the specification of Periodic Pairs in CFX-Mesh.

When you create a Periodic Pair, you supply two faces (or lists of faces) and a transformation which maps one face (or list) onto the other face (or list). The mesh on these two faces (or lists of faces) is then constrained to be identical.

So instead of modeling the entire -60 combustor can we cut out a 45 degree periodic wedge from the model and the mesh it using the above stated method of periodic meshing. The resulting mesh thus created is shown in **figure 3.4.** This reduces our computational domain to ¼ of the original domain. This would save a significant amount of computational time.

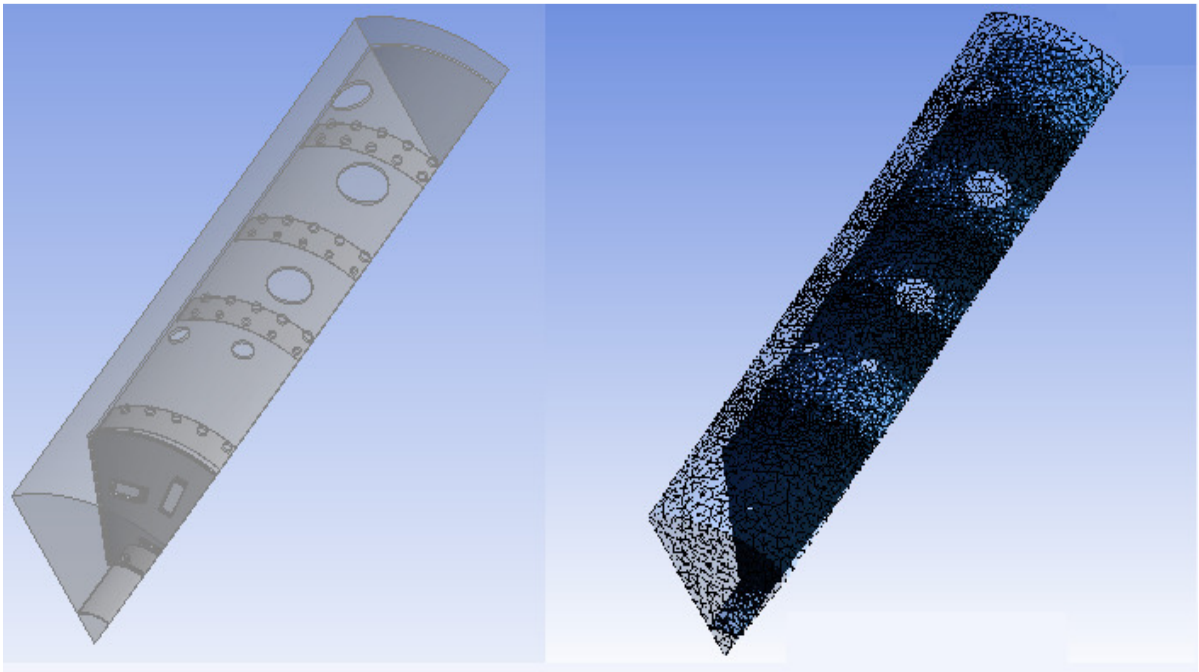

**Figure 3.4: The 45 degree wedge of the -60 combustor can and its mesh(right)**

## 3.3 Pre-Processing- defining the physics of the model and solver

This part involves setting up of the main CFD model. These include defining the fluid properties, the turbulence models, the boundary conditions, the domains and their interfaces and the chemical reactions and their kinetics. A number of options are available for each of these steps making it a very elaborate process to select every parameter very carefully according to our needs. CFX-Pre is the physics definition preprocessor environment for Ansys CFX. It is capable of importing 3D meshes and then setting up the required physics that need to be modeled. The files created by the pre processor are the input for the solver.

The Navier Stokes (NS) equations govern the fluid flow in the domain. These set of partial differential equations include the continuity, momentum and energy equations. In order to simulate combustion or other chemical reactions, additional equations are solved in conjunction with the NS equations. There are many approaches to discretize and solve the equations numerically. CFX solvers use the very popular finite volume method. In this method the domain is divided into discrete volumes. All the governing equations are discretized and solved for every finite element volume. The governing equations are integrated over all the control volumes. The governing equations are in integral form as we are using the finite volume method. These equations are then discretized using some scheme into a set of algebraic equations. These equations are then solved iteratively and as the solution approaches the exact solution it is said to converge.

As a result we get values of the flow field variables at the centroids of each control volume. Thus we get a complete picture of the flow field. The equations do not have an exact

analytical solution. Hence they are solved numerically in an iterative process. CFX uses ILU decomposition method to solve the set of the algebraic equations. Every iteration ends with an error or residual. These residuals exist for every control volume. In order to monitor the convergence of the entire problem the solver finds out the root mean square (RMS) value of this residual over the entire domain.

### 3.3.1 Turbulence modeling

The Navier Stokes equations govern both laminar as well as turbulent flows. However the length scales of the turbulent effects of the fluid flow are significantly smaller than the sizes of our finite volume elements. To resolve the turbulence effects in our model up to the Kolmogrov scale would mean very small finite volumes resulting in huge mesh sizes. Thus Direct Numerical Simulation (DNS) would require huge computational resources which are not available at present. However turbulence modeling is important as the flow variables depend quite heavily on them. In most of the applications we cannot neglect the effect of turbulence in the flow. Thus we have to use turbulence models to account for the effect of turbulence without resorting to highly fine meshes and DNS. Most of the turbulence models are based on statistical turbulence. We use Reynolds Averaged Navier Stokes (RANS) models to set up our CFD model.

If we are interested in looking into steady state solutions then we see that the time scales are much larger than the turbulent fluctuation time scales. We can express the flow field variable in two parts viz. the time averaged component and the fluctuating component. The original Navier Stokes equation is time dependent and unsteady. By introducing the 2 components as

a time averaged component and a fluctuating component we can express the NS equations in a form suited for steady state solutions. However this now introduces new variables in our equations. The variables are the average component and the fluctuating component. In order to close the system of equations so that we account for the 2 extra variables we use a turbulence model. In our simulations we use the k-e turbulence model.

### 3.3.2 Combustion modeling

In order to set up a combustion model first we need to set up a multi-component fluid for our domain. However this depends on the complexity and details of our model's chemistry. Combustion of fuels involves reactants and products. The reactants consist of oxidizer, fuel and a dilutant like $N_2$ in most cases. The products of combustion (for a HC) include water and carbon dioxide in case of complete combustion. However in reality owing to the high temperatures we have a number of radical species and other products like unburnt hydrocarbons, soot, ash and also intermediate species during the combustion process. Thus in order to set up a combustion model it is important to first decide on the number of species we want to consider in our chemistry model. It could range from 4 to 4000. This would also have a huge effect on the computational time and also adversely affects convergence as the problem becomes huge. If we do not consider the radical species in our analysis we over predict the temperature fields. Another factor in combustion modeling is the rate at which the species are reacting with each other. This is one of the most important factors that influence the flame shapes and lengths. A number of assumptions can be made to model the reaction

rates. The main models are eddy dissipation model (EDM), finite rate chemistry, flamelet models. Each of these models have their own assumptions and their own advantages and disadvantages. Also fuels like JetA do not have a specific chemical formula. They are modeled by surrogates that closely match their chemical kinetics. Some of the chemical kinetics are based on empirical relations and hence add to the inaccuracies.

This results in a large number of combinations that are possible to model the combustion process. We need to make a careful choice based on our application and our needs.

#### 3.3.2.1 **Eddy dissipation model**

The eddy dissipation model of combustion assumes that the chemical time scales are small as compared to the mixing time scales. The model assumes that the reaction rate may be related directly to the time required to mix reactants at the molecular level. In turbulent flows, this mixing time is dominated by the eddy properties and, therefore, the rate is proportional to a mixing time defined by the turbulent kinetic energy and dissipation. High Damkohler numbers are very typical of diffusion flames. The diffusion flames in gas turbine combustion are can be modeled very effectively using this model of combustion.

#### 3.3.2.2 **Flamelet model**

The Flamelet concept for non premixed combustion describes the interaction of chemistry with turbulence in the limit of fast reactions (large Damköhler number). The combustion is

assumed to occur in thin sheets with inner structure called Flamelets. The turbulent flame itself is treated as an ensemble of laminar Flamelets which are embedded into the flow field.

The Flamelet model is a non equilibrium version of the classical “Burke-Schumann” limit. It adds new details to the simulation of combustion processes compared to other common combustion models for the price of the solution of only two scalar equations in the case of turbulent flow. An arbitrary number of intermediates may be specified as long as their laminar chemistry is known.

The main advantage of the Flamelet model is that even though detailed information of molecular transport processes and elementary kinetic reactions are included, the numerical resolution of small length and time scales is not necessary. This avoids the well-known problems of solving highly nonlinear kinetics in fluctuating flow fields and makes the method very robust. Only two scalar equations have to be solved independent of the number of chemical species involved in the simulation. Information of laminar model flames are pre-calculated and stored in a library to reduce computational time. On the other hand, the model is still restricted by assumptions like fast chemistry or the neglecting of different Lewis numbers of the chemical species.

The coupling of laminar chemistry with the fluctuating turbulent flow field is done by a statistical method. The PDF used can in principle be calculated at every point in the flow field by solving a PDF transport equation as shown by Pope and many others. The most often

mentioned advantage of this method is that the non-linear chemical source term needs no modeling. Even though the method avoids some modeling which is necessary if using moment closure, it still requires modeling of some of the most important terms, in particular, the fluctuating pressure gradient term and the molecular diffusion term. If combustion occurs in thin layers as assumed here, the molecular diffusion term is closely coupled to the reaction term and the problem of modeling the chemical source term is then shifted towards modeling the diffusion term.

However, there is no source term in the mixture fraction equation, which is the principal transport equation in the Flamelet model. Therefore, a presumed beta-PDF, which is a commonly accepted choice, is used here. Additionally, this avoids the extremely large computational efforts of calculating the PDF in 3D with a Monte Carlo method.

The following list outlines the assumptions made to derive the Flamelet model:

- Fast Chemistry
- Unity Lewis numbers for all species
- Combustion is in the Flamelet Regime
- Two feed system, that is, fluid composition at boundaries must be pure “fuel,” pure “oxidizer” or a linear blend of them.
- Diffusion flames

The CFX-RIF flamelet generator was used to generate the flamelet libraries.

#### 3.3.2.3 **NOx emission modeling**

Due to the stringent emission norms imposed on modern gas turbines it is very important that the CFD model is capable of predicting the NOx emissions. Three types of NOx formation mechanics were considered: Thermal NOx, fuel NOx and prompt NOx. Out of all these the most dominant was the thermal NOx. The post processing technique was used to process the NOx formation. Thermal NOx occurs mainly due to high temperatures causing O radicals to react with $N_2$ to form NO. Thus if we know the temperatures we can find out the concentration of O radicals from $O_2$ concentration. A scaled down reaction mechanism is developed in CFX reaction library that gives the rate of NOx formation for a given temperature and $N_2$ and $O_2$ concentrations. Generally the concentration of NO is of the order of PPM in the combustion products. This small amount of NOx does not affect the bulk properties of the fluid. This gives us the opportunity to model NOx via post processing. Thus after the run is complete we have the solution fields for temperature and $N_2$ and $O_2$ mass fractions. Using all these parameters the NOx field can be solved. It has been observed that post processing of NOx give more accurate results than setting up a separate reaction and solving for its transport equations.

## 3.4 Post Processing- flow visualization

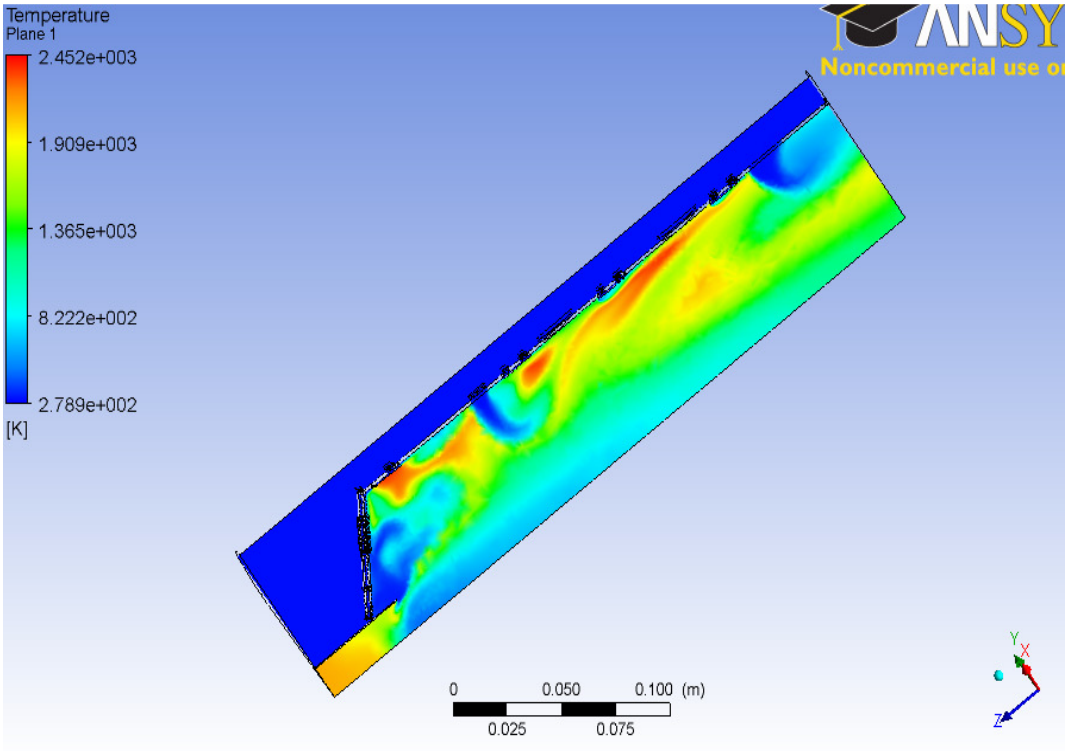


**Figure 3.5: Post processing of results using CFX-Post**

The post processing of the solutions were done using CFX post. Slice planes, contour plots, surface streamlines, 3D streamlines were used to get a visualization of the flow and the flow field variables.

# Chapter 4

## CFD analysis of combustor with swirl vanes

The aim of the current work is to burn a viscous fuel inside a combustion chamber. Flame stability is crucial for combustion in any device. Previous research [7-13] has shown that flame stability can be achieved through bluff body or swirl stabilization. A lot of research has effort has been directed towards this but swirling flows coupled with combustion are poorly understood. The studies [7-13] show that a swirling flow is capable of creating a vortex and its breakdown. This vortex breakdown creates a recirculation zone. The critical parameter which governs this vortex breakdown is the swirl number. Vortices break down if the swirl number is greater than 0.6 [14]. The swirl thus results in reduction of the flame lengths due to the entrainment of the fluid within the recirculation zones and improves flame stability as a result of the creation of toroidal recirculation zones [7-12].

Swirl can be introduced into the flow by two methods, by using guide vanes or by tangential entry of fluid into the fluid stream. In this design we use guide vanes.

### 4.1 Air inlet and fuel injector

In order to limit the number of specialized components for the retrofit burner, we attempted to use the air swirl vanes and fuel injector from a GTCP85-98D combustor can, a turbine system from the same family as our GTCP85-397 system. This would allow us to minimize

differences between our combustion chamber and the combustion chamber currently utilized by the GTCP85-397 gas turbine while ideally maintaining similar fluid physics. The air swirl component is about 6.5 inches in diameter with 6 primary rectangular swirl vanes around the fuel injection nozzle. Also surrounding the fuel injection nozzle are several smaller swirl vanes. This air swirl plate is pictured in the following **figure 3.2**.

As seen in figure 3.2, the fuel injection is through a single nozzle located along the center axis of the swirl plate. This allows the fuel to spray directly into the swirling inlet air. The fuel injector line was designed to have a T-fitting and valves prior to the nozzle that would allow Jet-A and glycerin flow through a common pressure atomizing nozzle. Combustion experiments with the 98D swirl plate allowed us to make several observations. First, we found that our system was capable of burning Jet-A over a wide range of flow rates. The design implemented is shown in the Figure 4.3. This swirl plate is fixed on the burner plate and connected to the bleed air port as discussed earlier in 2.4. The test stand has a burner plate and the ceramic liner sits over that burner plate. The idea is to create a swirl stabilized diffusion flame. The swirl vanes would create a highly swirling flow in the chamber. The vortex breakdown would result in the formation of recirculation zones.

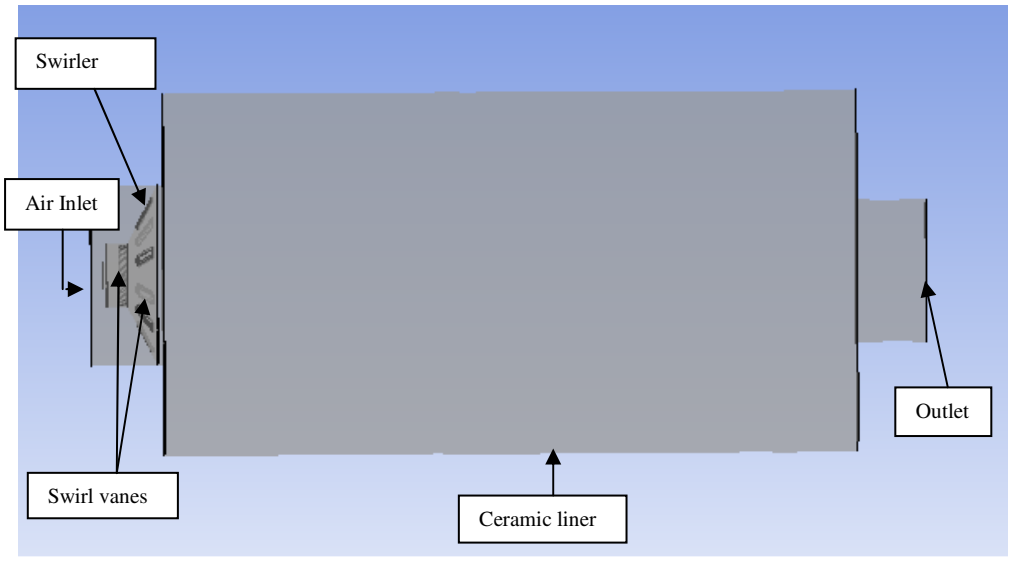


**Figure 4.1: Initial burner design with swirl vanes**

## 4.2 Combustor liners

The initial combustor liner dimensions were based on previous research performed at the Applied Energy Research Lab. The combustion chamber in this previous work had a length of 12 inches and an inner diameter of 6 inches. The combustor liner diameter selected for the gas turbine retrofit was 12 inches, while the length was a proportional 24 inches in length. The significant increase in the combustion volume is to account for the increased mass flux of fuel and air compared to the previous system. Unfortunately, the narrower chambers would have higher velocities and produce longer flames, and more importantly less residence times. To this end, we selected further investigation with the 24 inch long, 12 inch inner diameter chamber, as it was capable of burning glycerin.

**Figure 4.2: Comparison of different liner geometries**

## 4.3 CFD results for swirl vane design

The model developed in Chapter 3 was used to study the performance of the above design. The entire geometry was accurately modeled in full 3D using SolidWorks and Ansys DesignModeler. Special attention was given to the measuring the minute details of the swirl vanes. The vane angles have a large impact on the flow patterns, especially the swirl. The resulting solid model was then meshed using the CFX Mesh. The mesh consists of 483268 nodes. In order to specify well posed boundary conditions the inlet to the combustion chamber had a boundary condition of mass flow rate of the incoming air and the exit pressure was specified at the outlet of the combustion chamber. These boundary conditions are the most robust of all possible combinations. The walls of the combustion chamber had a no slip

and adiabatic boundary condition. Source points were used to introduce fuel into the domain. The following simulation was for an equivalence ratio of 1. The eddy dissipation model was used for simulating combustion. The following results were obtained after the solution converged and met its convergence criterion.

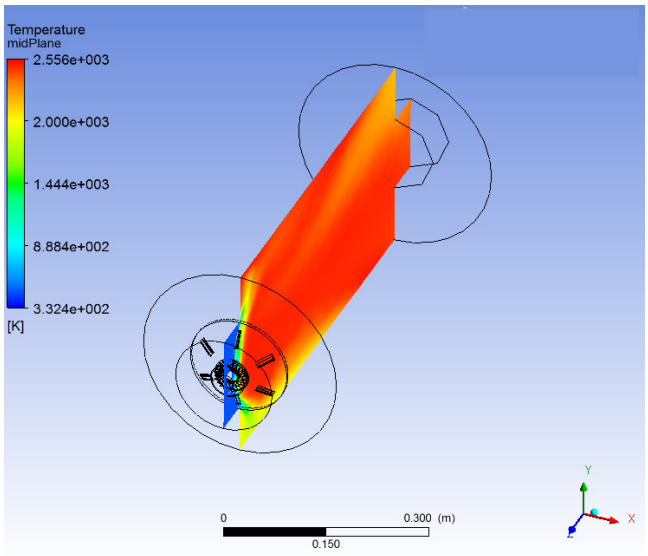


**Figure 4.3: Plane YZ for flow visualization.**

We get the results for the entire 3D flow field. In order to visualize the flow and to compare different cases we look at the YZ plane and the flow field variables in that plane. This view gives us an idea as to what is happening throughout the combustion chamber right from the inlet to the exit. We would use this plane as the reference plane for comparing different models and simulation results.

### 4.3.1 Flow pattern

The streamlines from Figure 4.4(a) and 4.4(b) below clearly indicate the vortex breakdown resulting from the swirl induced by the swirl vanes. The recirculation zones are clearly visible and are according to our expectations. The incoming air from the inlet passes through the swirl vanes and a rotational motion is imparted to it. Due to the centrifugal forces the fluid has a tendency to move away from the center and towards the walls. This creates a relative low pressure at the center and a higher pressure at the circumference. When this pressure difference is high it causes the low pressure central zone to create a flow from the high pressure region towards the lower pressure region. This sets up the recirculation zone.

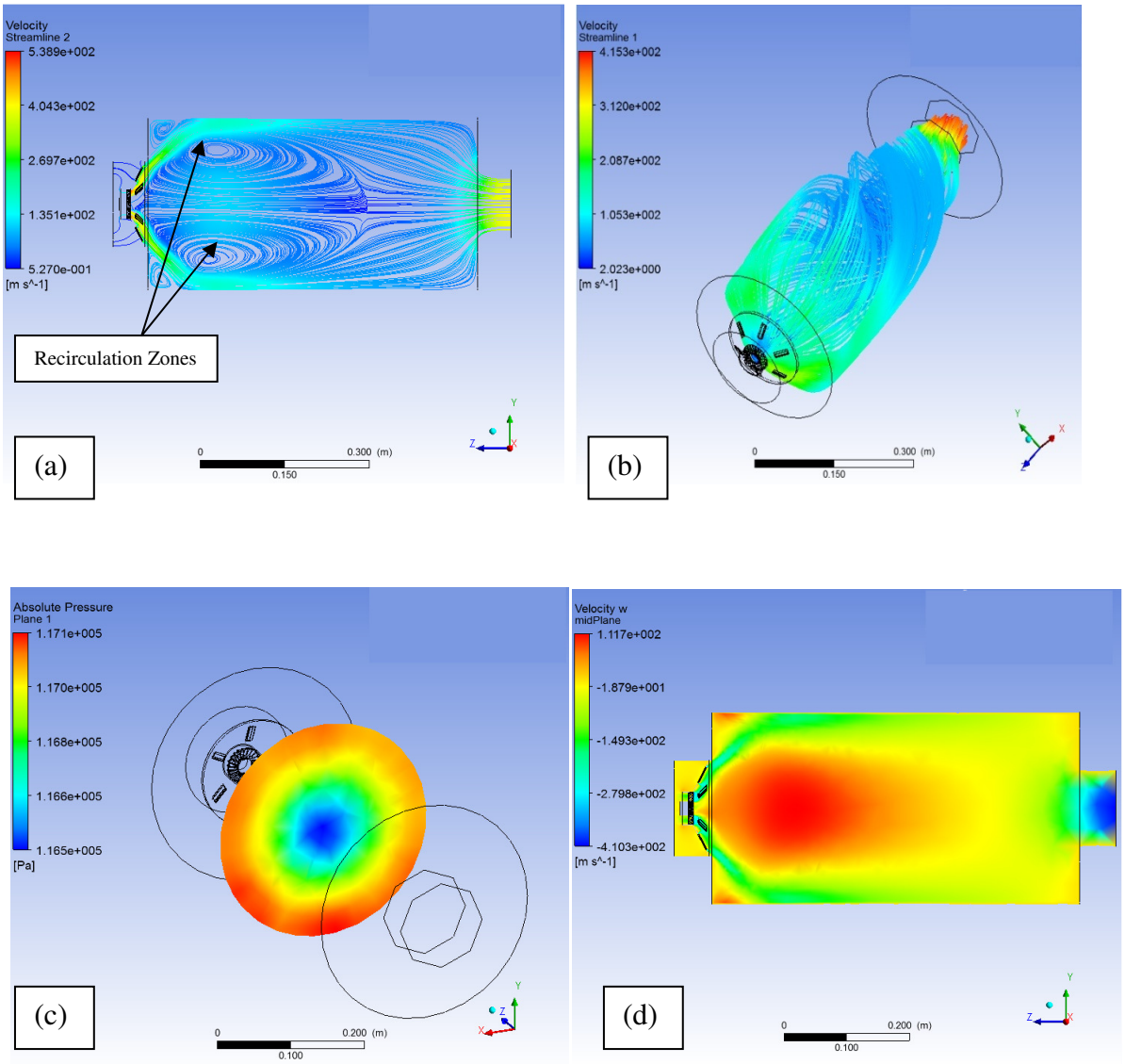


**Figure 4.4: (a) Surface streamlines (b) 3D streamlines (c) Pressure Contours on XY plane (d) Velocity(in Z dir.) contour**

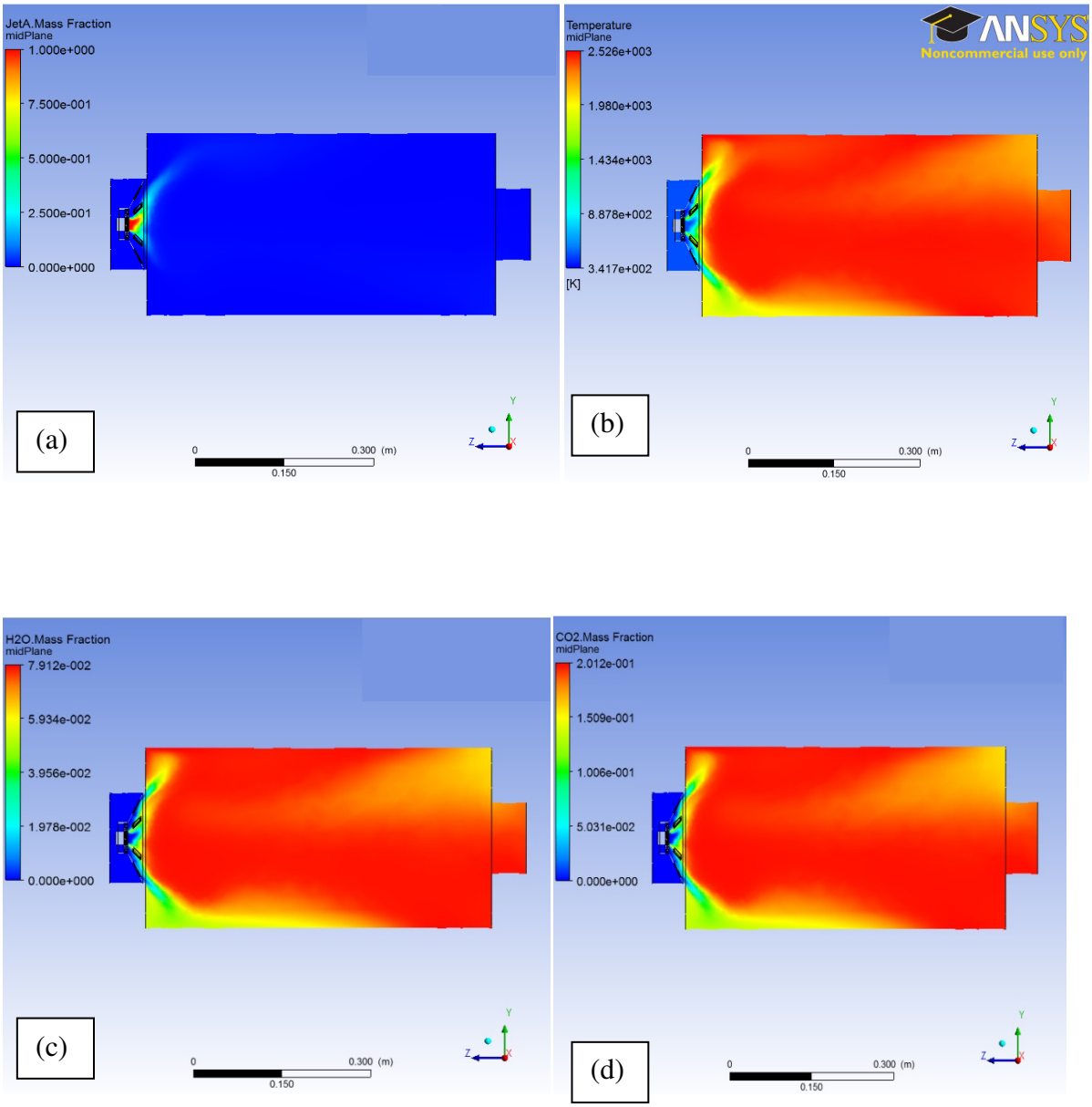


**Figure 4.5: (a) Fuel Mass fraction (b) Temperature profile (c) $H_2O$ mass fraction (d) $CO_2$ mass fraction**

From **Fig. 4.5(a)** we can see the injection of Jet-A fuel into the domain. Jet-A has been modeled in gas phase and the entire simulation involves only gas phase. We see that the fuel injected gets trapped in the recirculation zones that are created by the swirl. The equivalence ratio is 1 and as expected we observe that the entire mass fraction of fuel is being consumed by the combustion process. The mass fraction of oxygen is 0 after the combustion zone. We observe a case of complete combustion and that the flame is perfectly stabilized owing to the re-circulation zones. The recirculation zones have appeared as we had expected, just after the swirler plate exit and at the root of the fuel injection. However these are very ideal conditions. The simulation is still far away from reality as we know that the fuel in liquid phase will behave very differently as compared to a fuel in the gaseous phase. The eddy dissipation model assumes that the fuel reacts with the oxidizer spontaneously as soon as it is mixed with it i.e. Damkohler number is very large. However in reality there is some delay in the ignition process. This delay could change the entire flow dynamics. Moreover in the experimental results the flame that was observed visually was quite different. The experimental setup could burn Jet-A for a wide range of flow variables. In the next simulation an ignition delay was implemented for Jet-A and the results were observed.

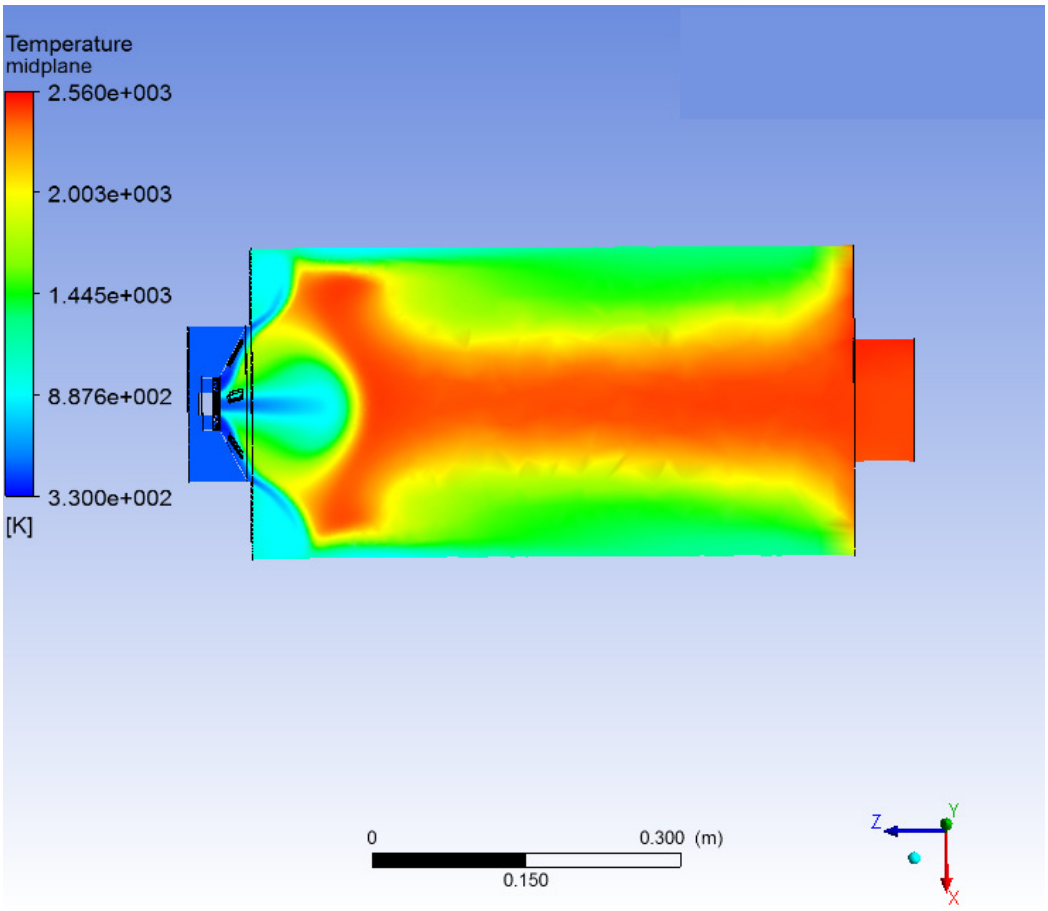


**Figure 4.6: Temperature profile with ignition delay**

In Fig. 4.6 we see that the temperature profile is completely different from the profiles that we see in Fig. 4.5(b). The flame that was observed in the experiment had very close resemblance to the one we see in Fig. 4.6. A column of hot gases and swirling flame was seen rising from the bottom towards the exit of the combustor. This result basically prompts us to investigate into the fact that assuming Jet-A to be in gaseous phase will have significant errors in our flame predictions. Experimentally it was also observed that after the system was

preheated with Jet-A and when it was switched over to glycerin the system could not burn any glycerin. This was a motivation for investigating the effects of a liquid spray.

## 4.4 Liquid spray simulation results

The evaporation process of a liquid is governed and modeled by the Anotine equation in CFX. Data for evaporation of liquid jet-A was available from the CFX material library. The simulation was set up with the same boundary conditions except for the fuel injection. A multiphase simulation was set up to model the evaporation process of the liquid fuel. The following results were observed for liquid jet-A spray.

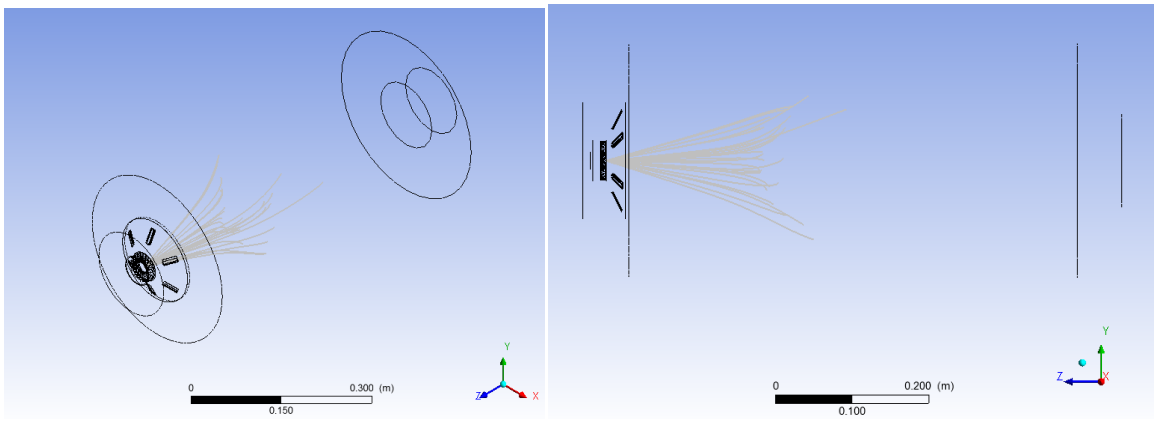


**Figure 4.7: Liquid Jet-A spray pattern**

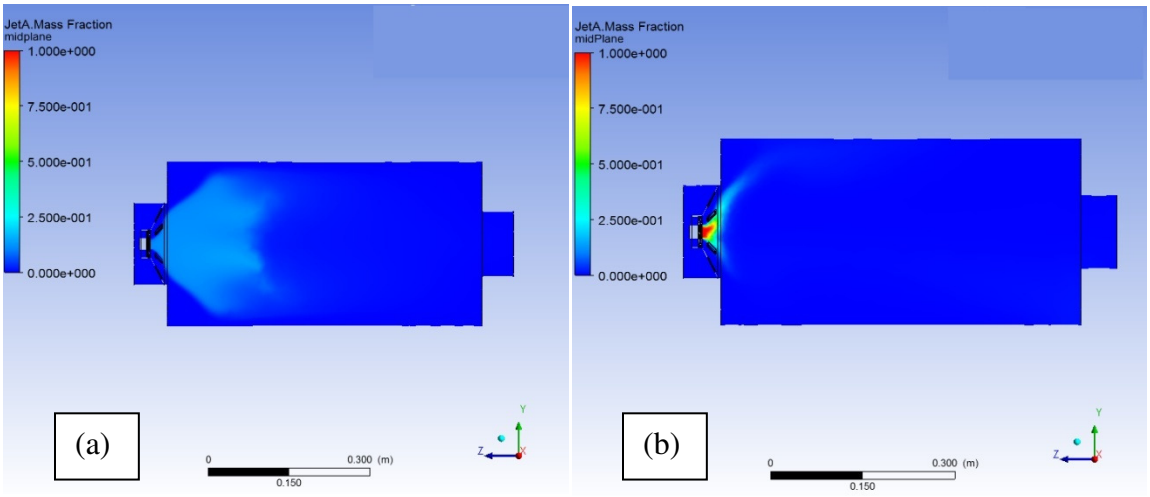


**Figure 4.8: Fuel mass fraction contour for: (a) Liquid spray (b) Gas phase fuel injection**

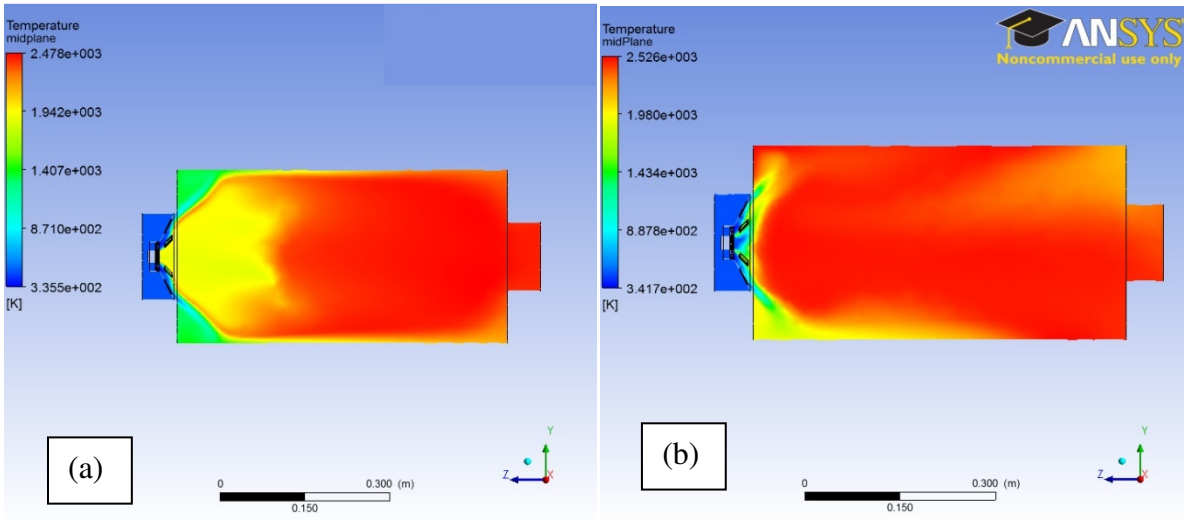


**Figure 4.9: Temperature contour for: (a) Liquid Jet-A spray (b) Gas phase Jet-A**

From Figs. 4.8 and 4.9 it is clearly evident that the flame lengths are much longer for the liquid spray. The liquid particles have much higher momentum than gas. Thus they are not entrapped inside the recirculation zone and a large part of them can escape the recirculation zone. Thus we get a lift off of the flame. The CFD model however clearly demonstrates that complete combustion occurs while burning Jet-A. This was also validated by the experimental results. We were able to burn over a wide range of mass flow rates of air. However after preheating the chamber with Jet-A when glycerin was injected into the chamber it was found that the flame could not sustain itself. After a few seconds the flame ceased to exist and blew off. White smoke was seen coming off the exhaust. This was mostly glycerin getting decomposed into acrolein due to incomplete combustion. This needed to be investigated. However there is no data available for gas phase and combustion kinetics for glycerin. Glycerin has much higher values of enthalpy of evaporation when compared to Jet-A. The following vapor pressure curves [15-16] demonstrate this difference.

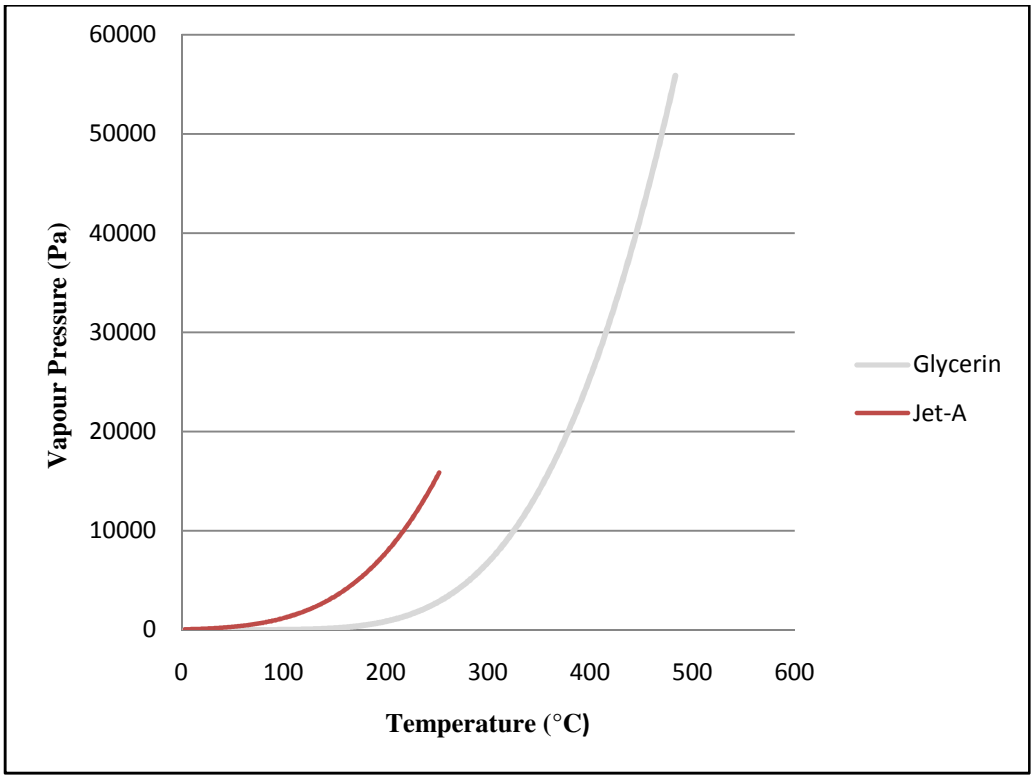


**Figure 4.10: Vapor pressure curves from Anotine equation**

Thus we see that there is a difference in the vapor pressure by an order of magnitude. Combustion occurs in gas phase only. As long as the fuel stays in its liquid phase it does not react with oxygen. This could be a major reason for not being able to burn glycerin in this set up.

It was argued that the evaporation and mixing time scales of glycerin are much higher than the chemical time scales of combustion i.e. Damkohler numbers are very large. Thus if we can approximate the evaporation process of glycerin and use the same combustion and gas kinetics model as that of Jet-A we can get a fair amount of insight into glycerin combustion. The Anitone equation coefficients were modified for the evaporation process to that of

glycerin and the simulations cases were run. The boundary conditions and meshes remained the same. The change was the rate of evaporation. The following results were observed.

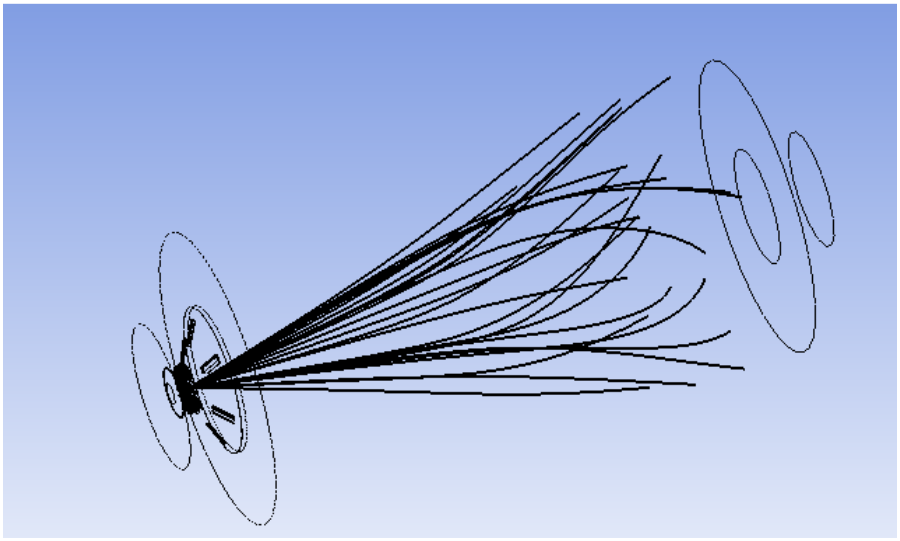

**Figure 4.11: Glycerin spray pattern**

Here we see that the sprays are much longer for glycerin as compared to the Jet-A spray in figure 4.7.

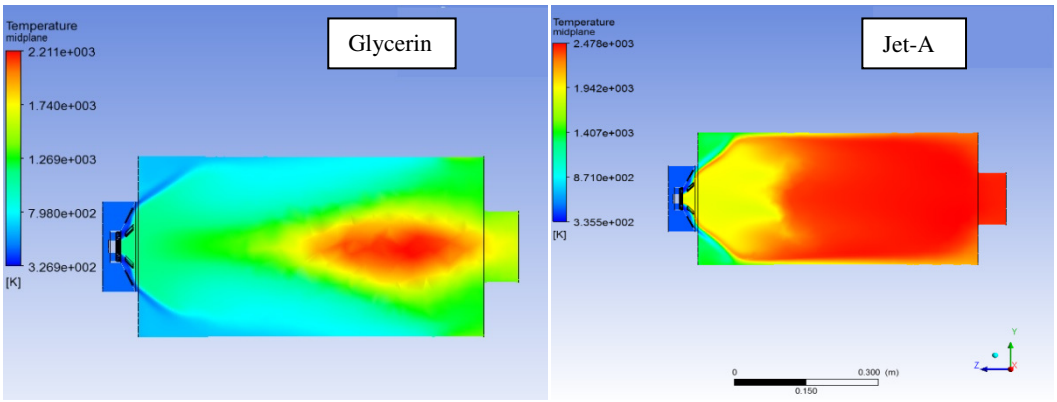


**Figure 4.12: Temperature profiles for glycerin and jet-A combustion.**

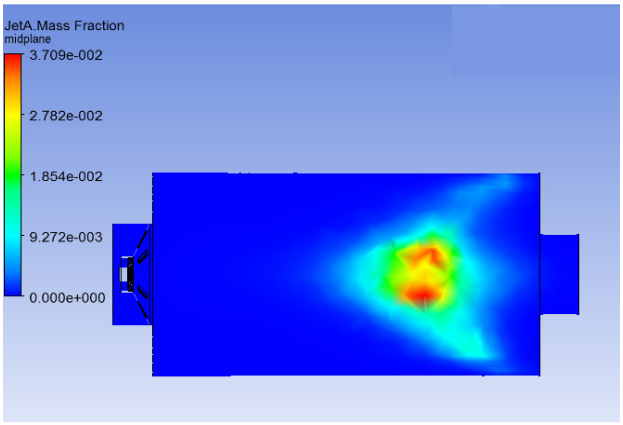


**Figure 4.13: Fuel mass fraction distribution.**

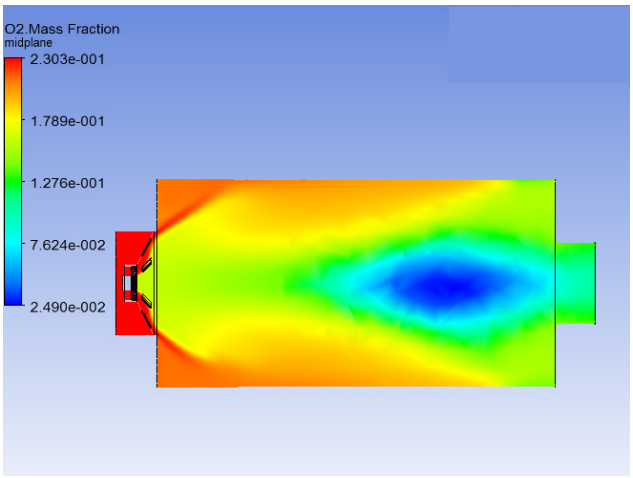


**Figure 4.14: Oxygen mass fraction.**

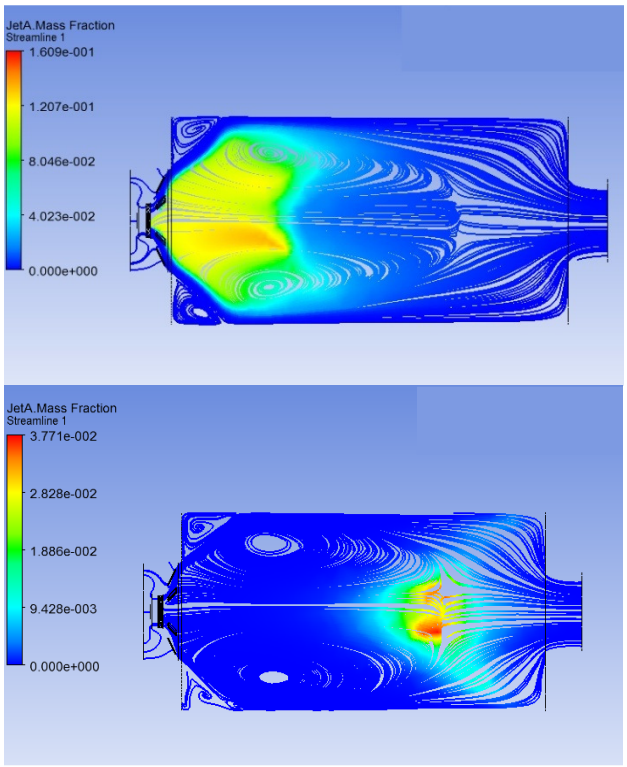


**Figure 4.15: Fuel concentrations on streamlines**

The results clearly show the inability of the system to burn glycerin effectively. When we compare these results to the results that were obtained for jet-A spray we can clearly see the differences in the two cases. The Jet-A spray evaporates quickly within the confinements of the combustion chamber. This is however not the case in the glycerin spray. Owing to the high enthalpies of vaporization we see that the spray lengths are longer. The liquid glycerin particles take longer time to evaporate. Combustion will occur only when the particles reach the gas phase. This delay is the main reason for the system's inability to burn glycerin. Thus even though we are not able to burn glycerin in this setup we were able to burn Jet-A. Figure 4.15 clearly shows how the Jet-A fuel particles get entrapped inside the recirculation zones where as the glycerin spray escapes them resulting in incomplete combustion. The CFD model was validated and could correctly predict the blow out of the flame. This design was also integrated with the plenum to see if that would help in burning the viscous fuel.

## 4.5 Final Integration of design with plenum

Ceramics are not capable of handling high pressures. We cannot have a combustion chamber made out of ceramics as most of the gas turbine combustion chambers operate under high pressures. Thus it was planned to have the ceramic casing inside a pressurized container such that the pressures on both sides of the ceramic wall are same. This would mean that hoop stresses would not develop within the ceramic. Gas turbines run at pretty low equivalence ratios. A typical gas turbine combustion chamber bifurcates air into primary and secondary air streams. The primary air stream is mixed with fuel within the flammability limits. After combustion of this mixture in order to bring down the temperature of the gases it is mixed

with the secondary air stream. The exhaust gas exit temperature from the combustion chamber is dictated by material constraints of the turbine. The maximum limit for most turbines till date is around 1000 °C. Moreover the combustion liner needs to be kept under certain maximum prescribed temperatures. The ceramic liner was meant for the purpose of primary air stream to mix with the fuel and burn the fuel completely. Then the secondary air stream would be mixed with the primary air stream coming out of the ceramic casing. This would bring down the overall temperature of the exhaust gases up to the desirable limit. The following design of integrating the plenum and ceramic casing was implemented. The gate valve shown in **Fig. 4.15** controls the bifurcation of primary and secondary air streams. When the gate valve is completely closed then the entire incoming air will go through the primary section through the ceramic. As we open the gate valve some air gets bypassed through the secondary section towards the exit. This secondary air then dilutes the combustion products.

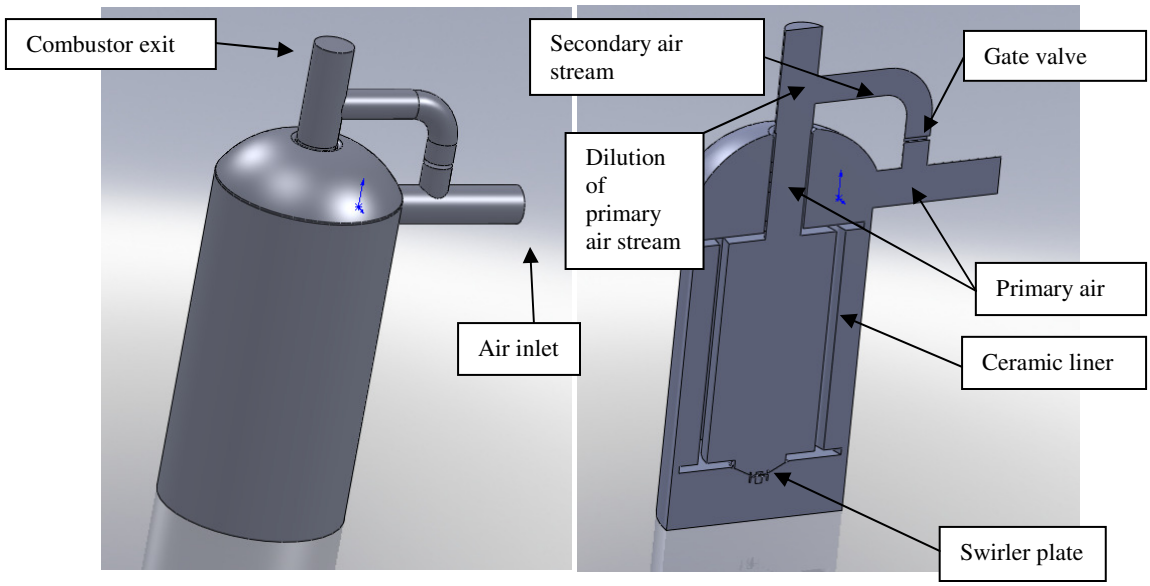


**Figure 4.16: Integrated design with plenum (left) and its cross sectional view (right).**

In the experiments it was observed that the section of the combustion chamber that connected the plenum to the top plate of the ceramic casing had melted. The reasons for this disaster were not very clear. The overheating of the exit tube could have been caused by a number of reasons. Initially it was thought that the equivalence ratios were not properly set and this would have resulted in its failure. Another theory was that the welds that connected the exhaust pipe and the top plate of the ceramic could have given off. This would force the air to go through these holes and bypass the swirlers. Thus the combustion zone would have shifted upwards towards the exhaust pipe and melted the pipe. This case was modeled using the CFD model. In order to simulate the failing of the welds 4 holes were made into the solid model as shown in Fig.4.17.

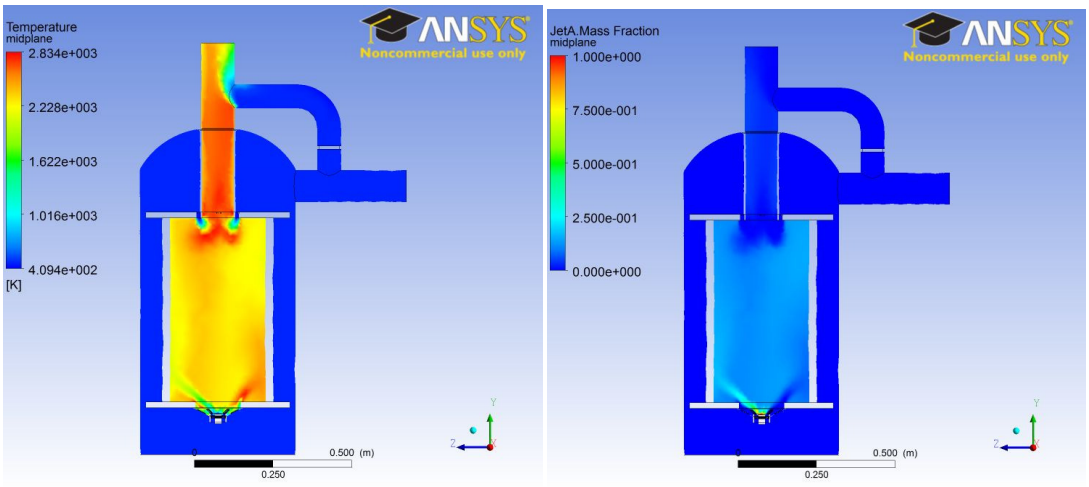


**Figure 4.17: Temperature and fuel mass fraction contours for damaged chamber.**

The results clearly show how the primary air stream is bypassing the swirlers. The combustion zone has shifted significantly upwards and also the temperatures at the welds have reached a point that would melt off the pipe. Thus failing of the welds could be a possibility for the failure of this design.

## 4.6 Reasons for failure and conclusions

Thus we see that this setup can burn Jet-A but fails to burn glycerin. Also the design failed completely when integrated with the plenum. The recirculation zones created by the swirler were not enough to create a reverse flow within the chamber that could entrap the glycerin particles. The low vapor pressure of glycerin resulted in longer spray lengths. Thus the results suggest that stronger recirculation zones are required to burn glycerin. The swirl vanes could provide a fixed quantity of swirl. There was no way to vary this parameter. Up to this

point the CFD simulations were performed in parallel and then the results were used to provide for an explanation. However once the CFD model was completely ready we can use this as a predictive tool. The CFD model clearly shows that this given design could not burn glycerin. Any future design could be tested on this CFD model before implementing it experimentally. This would greatly reduce the number of prototypes.

# Chapter 5

# Cyclone combustor design

## 5.1 New method to introduce swirl

The swirl vane design used in the previous combustion chamber had the disadvantage that the swirl produced could not be varied. Moreover the swirl was reduced greatly due to the fact that the retrofit combustion chamber had a much larger chamber diameter. There are a number of ways in which swirl can be introduced into the chamber. One way of imparting swirl through swirl vanes was used in the first design. The second way is to inject the air tangentially into the combustion chamber. This imparts a high rotational velocity to the fluid and creates the required swirl. The burners which implement this method of swirl induction are called cyclone burners. Cyclone burners have been typically used in applications which burn difficult to burn substances like vegetable oils, coal, and low grade solid fuels. This would be ideal for our application. The pattern of recirculation zones formed in this type of swirl induction is completely different from the swirl burners. Cyclone burners can have more than one (up to 3) concentric toroidal recirculation zones as compared to a single recirculation in swirl burners [13].

The new air and fuel inlet system was designed to address the challenges presented by the previous design. The new fuel injection system utilizes three pressure atomizing nozzles: a main Jet-A fuel nozzle that provides fuel during the pre-heat phase; a glycerin nozzle that

injects glycerin following the transition; and a pilot Jet-A nozzle that provides a small injection of Jet-A fuel during transition to glycerin to maintain a flame and to augment glycerin combustion when necessary. All three nozzles are located in the center of the burner plate. The new air inlet system was designed to be modular and allow as much control as possible over the fluid dynamics of the system. This was achieved by developing an air inlet system in which air entered the combustion chamber through 8 equally spaced one-half inch NPT pipes inserted into tapped holes that circumscribe the axis of the combustion chamber at a radius of 3.75 inches. The pipe fitting design was proposed because we could cheaply and quickly alter the fluid dynamics of the chamber with the multitude of NPT pipe fittings available. The new design was investigated in parallel utilizing both experimental and computational work. **Fig. 5.1** shows a configuration of the new air inlets, while **Fig.5.2** describes the three primary variables investigated with the new system.

**Figure 5.1: Air and fuel nozzles.**

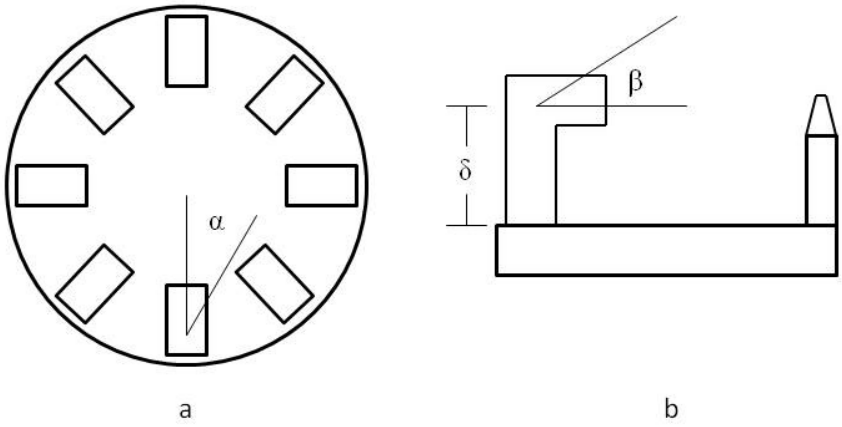


**Figure 5.2: Schematic of air nozzle orientation.**

## 5.2 Optimum air nozzle angle

Utilizing various NPT pipes and pipe fittings, we can adjust angles α and β as well as the distance δ from the swirl plate, allowing us to customize the flow physics. Typically all swirl burners have α=90°. However CFD simulations have now suggested that other values of α can have drastic effect on the flow and flames lengths. Simulations were run for values ranging from α=90° to α=0°. The eddy dissipation model and the flamelet model of combustion were used for the analysis. The following results were obtained from the EDM of combustion. For this model the periodic wedge approach was implemented. Since the domain consisted of 8 air nozzles a wedge of 45 degrees was implemented. The temperature profiles were an indication of the flame lengths. Mass flow rate at inlet was used along with pressure at exit as the boundary conditions. An equivalence ratio of 1 was used for all the cases.

Source points were used for fuel injection. All the simulations were gas phase. This was to get a general overview of the design.

### 5.2.1 EDM results

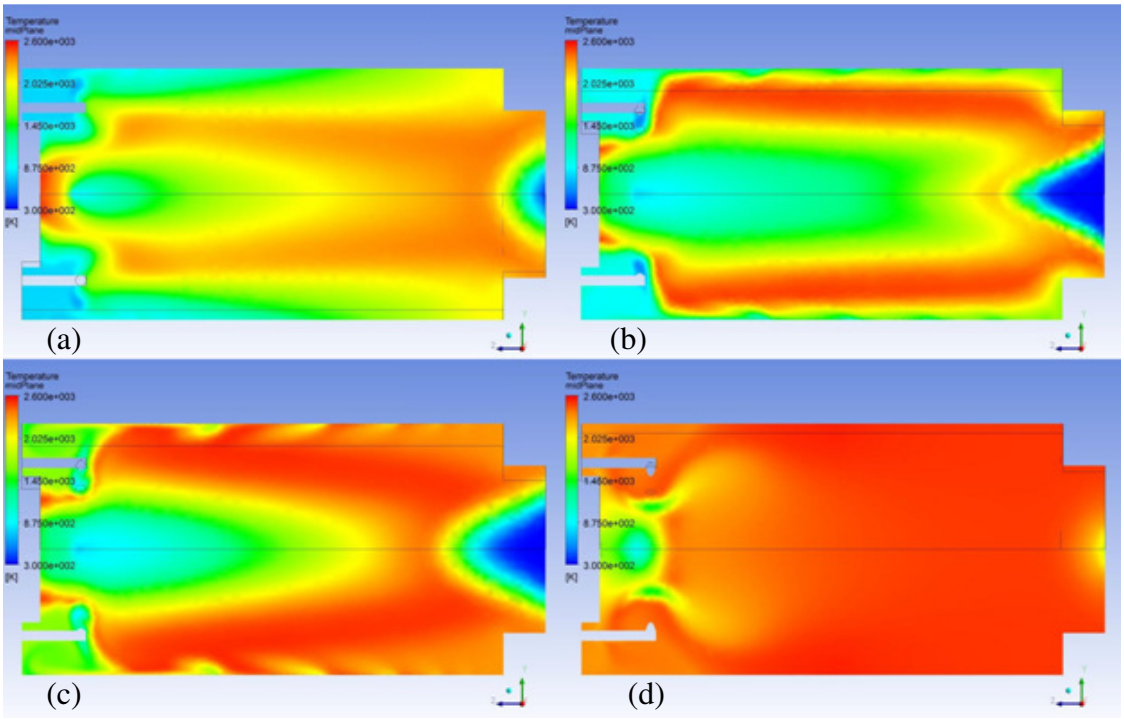


**Figure 5.3: Temperature plots obtained using EDM model (a): 90 deg. nozzle, (b): 52.5 deg. nozzle, (c): 42.5 degree nozzle, (d): 22.5 degree nozzle.**

We observe that the flame length decreases drastically for values of α=90° to α=20°. This indicates that the strength of the swirl increases drastically as we change the air nozzles from 90 towards 20. The same trends were also reported from the flamelet model of combustion. The flamelet model also gave us additional information on intermediate species. The intermediate species like O, OH, $OH_2$ give us an idea of the location of the combustion zone.

Thus we now know that the tangential air feed at α=90° is not as efficient as the lower values of α. This was valuable information on the design that the CFD model was giving us.

### 5.2.2 Flamelet model results

Here a comparison is done between the conditions when α is varied from 90° to 0°. These simulations also predict similar trends as the EDM model. The models were tested for α=90°, 50°,40°,20°,10°,5° and 0°.

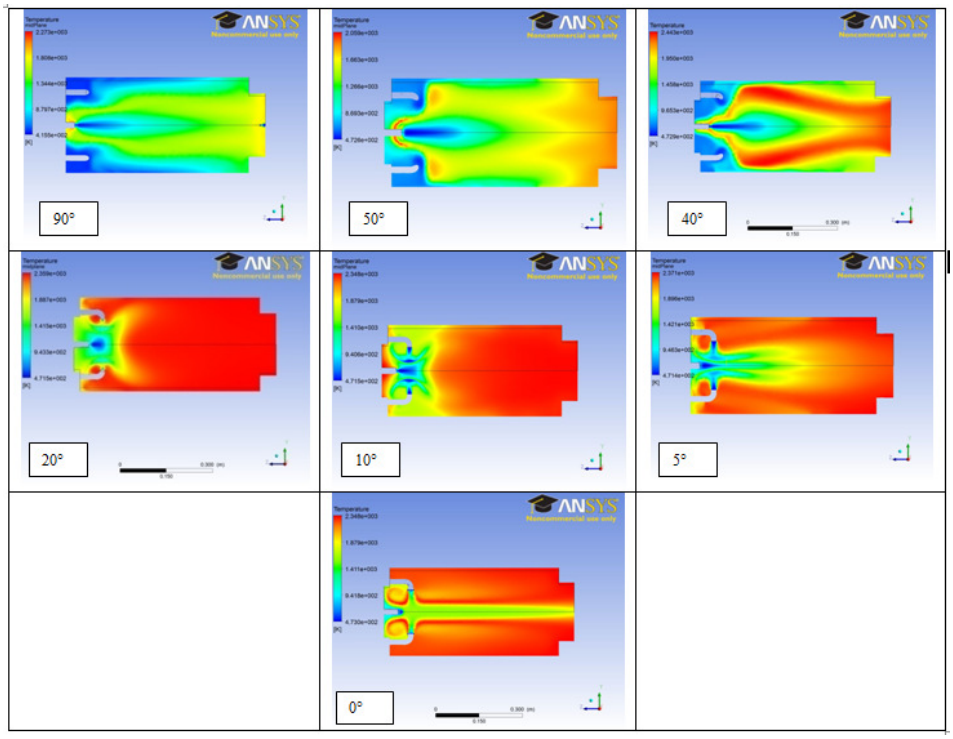


**Figure 5.4: Temperature contours for different nozzle angles obtained using the flamelet model.**

The trends seen from the EDM model are confirmed on the flamelet model as well. We see that the flame length goes down as we move from 90 to 0 degree. The zero degree case result is non –realistic as that would be a definite case of blow out. RANS models cannot simulate a blowout. This trend seems very useful to us to strike a stable a short length flame. The next steps of the analysis give some insight into these trends and their reasons of occurrence.

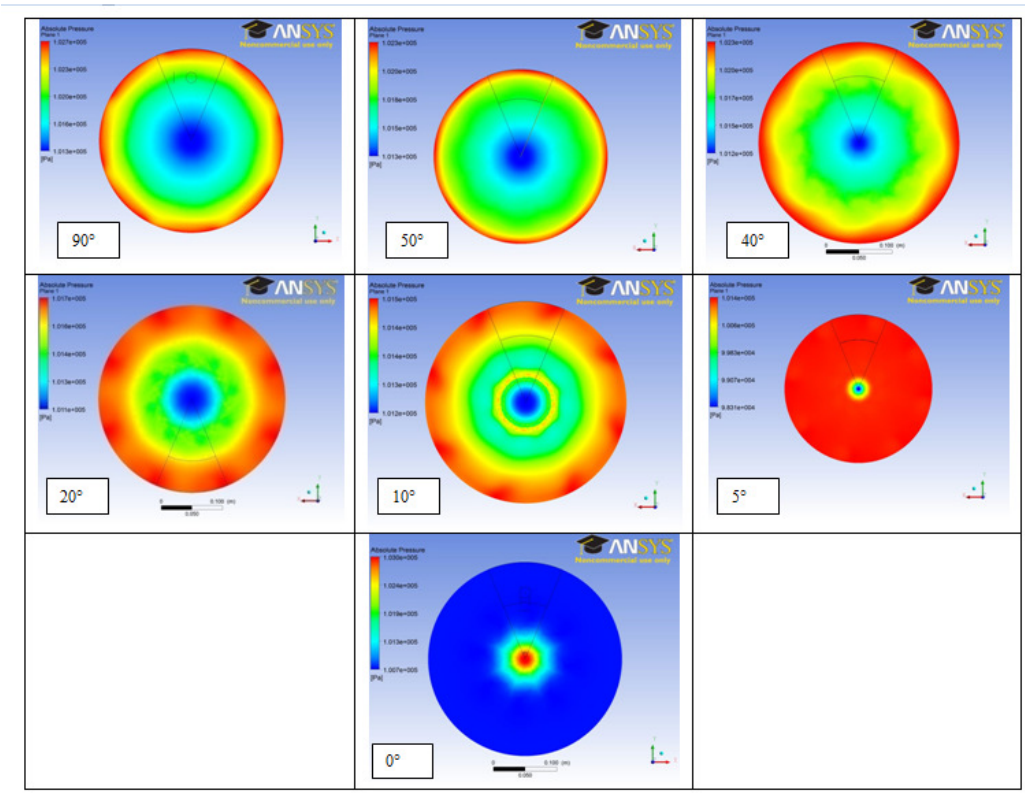


**Figure 5.5: Pressure contours for different nozzle angles obtained using the flamelet model.**

From the pressure contours it is very clear that as we move from 90 to 0 degrees the pressure in the central part of the combustion chamber goes down. The gradient in pressure drop

increases up to the 5 degree case. After that we see a reversal of the trend. The higher the gradient, the stronger the recirculation zone would be.

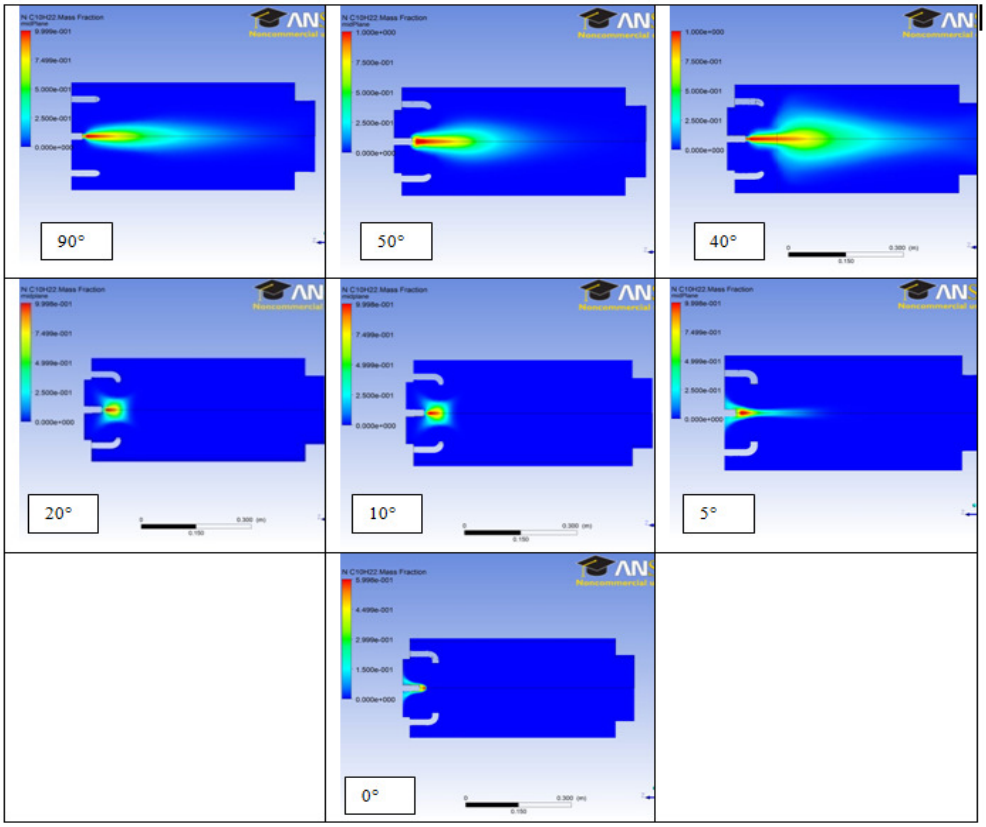


**Figure 5.6: Fuel mass fraction contour for different nozzle angles obtained using the flamelet model.**

The fuel mass fraction contours give a better idea of the process. It is very clear that as we are decreasing the angle of the air nozzles the fuel entrapment in the recirculation zone improves. The 90, 50 and 40 degree cases show how the fuel is spread across the chamber. The corresponding temperature contours are a result of this. The temperature would increase in the regions where the fuel gets consumed by the oxidizer.

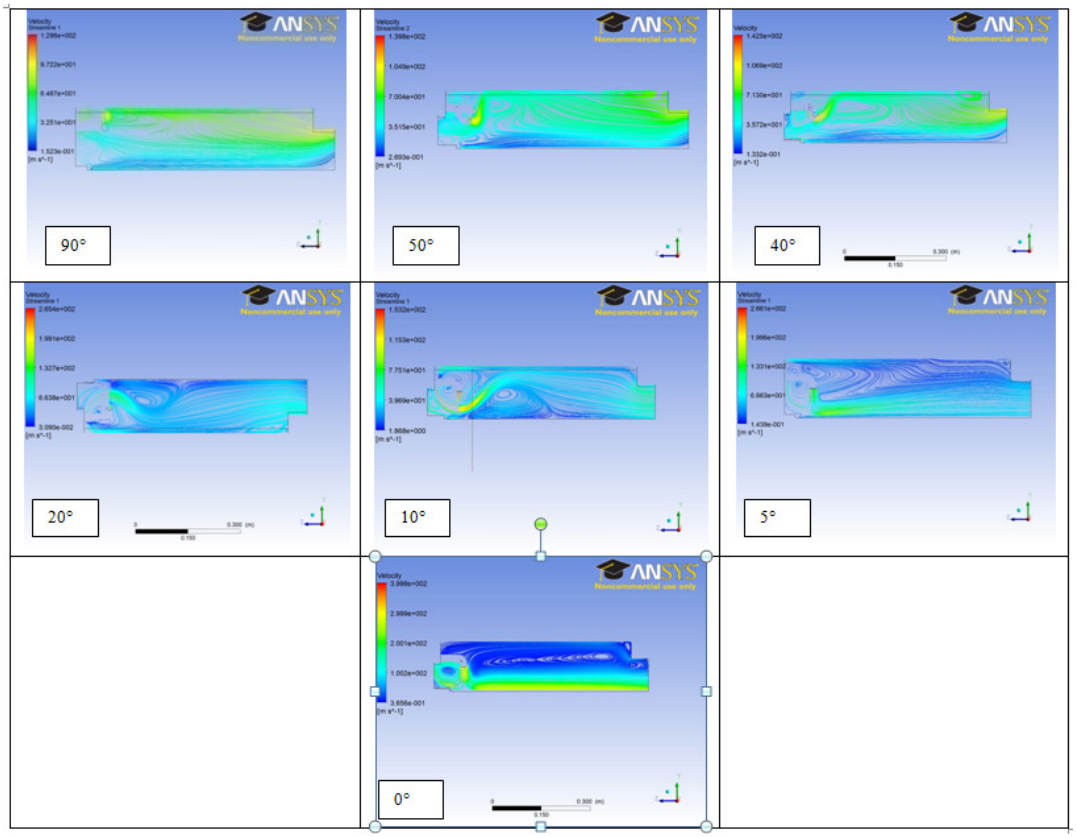


**Figure 5.7: 2D streamlines for different nozzle angles obtained using the flamelet model.**

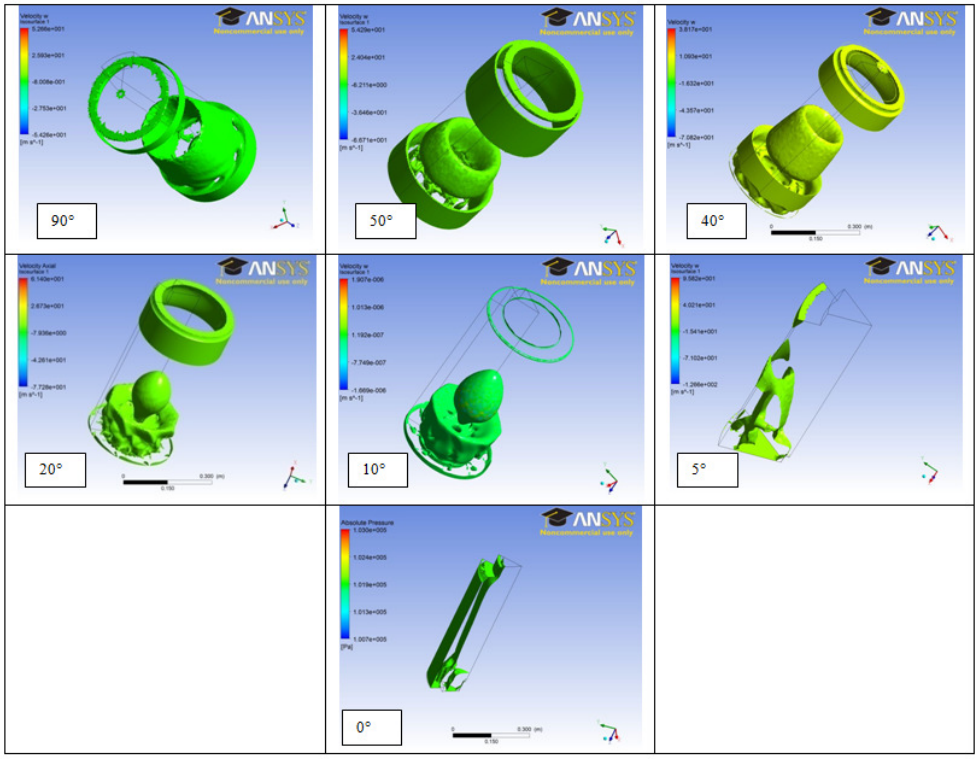


**Figure 5.8: Recirculation zones for different nozzle angles obtained using the flamelet model.**

Now from the 2D streamlines on the mid-plane we get an understanding of how the recirculation zones are developing. The strong vortex breakdown for case 20 and case 10 show that these configurations are ideal for shorter flame lengths. The high swirl creates longer residence times and we observe reduction in flame length. We can conclude that the 20 – 10 degree range is the best possible nozzle configuration for this geometry. These results were also verified experimentally. When the air nozzles were placed at 20 degrees the flame lengths obtained were significantly smaller. First α=90° configuration was fired on Jet-A. The system could burn Jet-A in this configuration. After the system was preheated and switched over to glycerin the flame could not be sustained after a few seconds. Thus this

configuration was not able to burn glycerin. The reason was same, insufficient residence time to evaporate the fuel. However now we had an idea that the swirl would be much higher for $\alpha=20°$. When this configuration was implemented it was observed that the Jet-A flame length was much smaller as compared to $\alpha=90°$ configuration. After pre heating the system the switch over to glycerin was made. In this configuration we were able to sustain the glycerin flame and this was the first time that glycerin was burnt successfully in this experimental set up. The combustion of glycerin was stable for the entire duration of the experiment, which was stopped after about 40 minutes. Several observations and subsequent changes were made upon examination of the burner after this test. It was discovered that all three of the fuel nozzles had melted. This was due to the intensity of the recirculation zone in close proximity to the fuel nozzles combined with the material limits of the brass pressure atomizing nozzles. To address these issues with the burner, we made several modifications. Cooling jets for the fuel nozzles were created by drilling holes in the burner plate that allow for compressed air to be directed at the nozzles. Next, the brass nozzles were replaced with stainless steel pressure atomizing nozzles. Finally, we varied $\beta$ and $\delta$ on alternating air inlets, while keeping the other four air inlets at the prescribed position. This allowed us to push the flame further away from the nozzles while maintaining the recirculation necessary for sustaining glycerin combustion. After some experimentation with these variables, a final design was selected for the retrofit combustion chamber, which is described in detail in the following section.

## 5.3 RQL technique implementation

Gas turbines typically burn very lean mixtures. These equivalence ratios are outside the flammability limits. In the past three decades the Rich burn, Quick Mix, Lean-burn combustion technique has gathered a lot of importance in stationary and mainly aero gas turbines. This technique is aimed at reducing the NOx emissions without compromising on flame stability.

Now as shown in previous experiments and simulations we can use the air nozzles in the 20 degree configuration. However this configuration can burn at equivalence ratios within the flammability limit only. However the need is to burn at equivalence ratios of 0.3. In order to have the global equivalence ratios below the flammability limits we adopt the following technique used in modern gas turbines. We have the primary air come in through the nozzles at the 20 degree configuration that ensures maximum swirl. In this region we ensure that the equivalence ratios are quiet high and the mixture ignites easily. Then we make use of the secondary air stream to dilute this mixture and bring down the overall equivalence ratio. The dilution zone (secondary air stream) should be located such that the combustion in the primary zone has completed.

## 5.4 Adapting RQL technique for use in ceramic walls

Implementing the technique discussed above would require us to drill holes in to the liner wall to force the secondary air stream inside the chamber. This was also observed in the

dash-60 combustor can. However this is very difficult to achieve with ceramic walls. Four of the holes are described by $\alpha = 22.5°$, $\beta = 0°$, and $\delta = 3$ inches, while the remaining four are described by $\alpha = 22.5°$, $\beta = 0°$, and $\delta = 12$ inches. The inlets alternate between these two configurations in a clockwise manner, as shown in **Fig. 12**. Also visible in this picture is the igniter between the air nozzles on the left. The igniter uses a high-voltage transformer to create a large voltage potential difference between the igniter rod and the grounded air inlet to create a spark.

**Figure 5.9: Modified air nozzles for staged air injection.**

## Combustor liner

The combustor liner is a cylindrical ceramic flue liner with an inner diameter of 12 inches, a wall thickness of 1 inch, and a length of 24 inches. The liner is shrouded in 2 inch thick insulation material and 0.05” steel. The steel sheeting is held in place using 4 stainless steel hose clamps. The combustion liner is held in place with a steel cap on the top of the liner that is three-quarters inch thick with an 8 inch hole. The cap is secured with 3 one-inch thick steel threaded rods which run vertically through the insulation material into the burner inlet plate.

**Figure 5.10: Combustor liner with insulation and steel sheeting.**

# Chapter 6

# Final Design

## 6.1 Integration with plenum

The high-pressure plenum was developed from a repurposed air compressor tank. The tank was a typical cylindrical pressure vessel with spherical ends. One spherical end was removed and welded to a 26 inch square three-quarter inch thick sheet steel section with a hole matching the diameter of the vessel to create a sealing surface. The vessel was made of quarter inch thick steel. Using Solidworks modeling software, the plenum was pressure tested to ensure its ability to withstand the gas turbine operating pressure with an acceptable factor of safety. The pressure vessel was also fitted with a pressure relief valve to prevent any significant over-pressure during operation. The pressure vessel encloses the combustion liner and seals against an identical 26 inch square steel sheet piece to which the burner plate and inlet air flange are also mounted. A very high temperature gasket is placed between these two plates. Twelve half-inch diameter bolts hold these plates together. The top of the plenum has a sight glass into the combustion chamber. The plenum exhaust line has two branches, each made of schedule 40 steel pipe and pipe fittings. The branches allowed us to study burning characteristics at a range of pressures as well as pre-heat the plenum without exhaust gases entering into the turbine if desired using a set of gate valves. The inlet to the turbine section required a specially designed 304 stainless steel adapter. The adapter allows for the combustion gases to enter the turbine while forcing the compressor air through the

combustion chamber. The adapter design mimics the combustion chamber cap of the original combustion chamber for the GTCP85-397 turbine that seals the system.

**Figure 6.1: High pressure plenum and turbine inlet.**

## 6.2 CFD results

The simulation test cases were set up for this geometry. The flamelet model of combustion was utilized. An equivalence ratio of 0.4 was used which was same as the experiments. In these simulations the NOx emissions were calculated by post-processing the thermal NOx formation.

### 6.2.1 Flamelet model and Jet-A in gas phase

In this simulation source points were used to inject gas phase fuel into the domain.

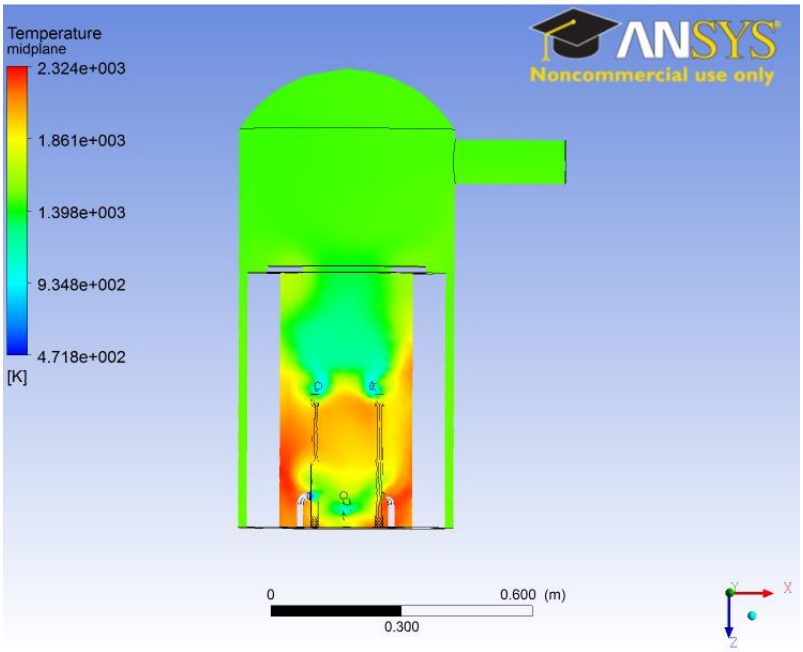


**Figure 6.2 : Temperature contour for gas phase Jet-A combustion**

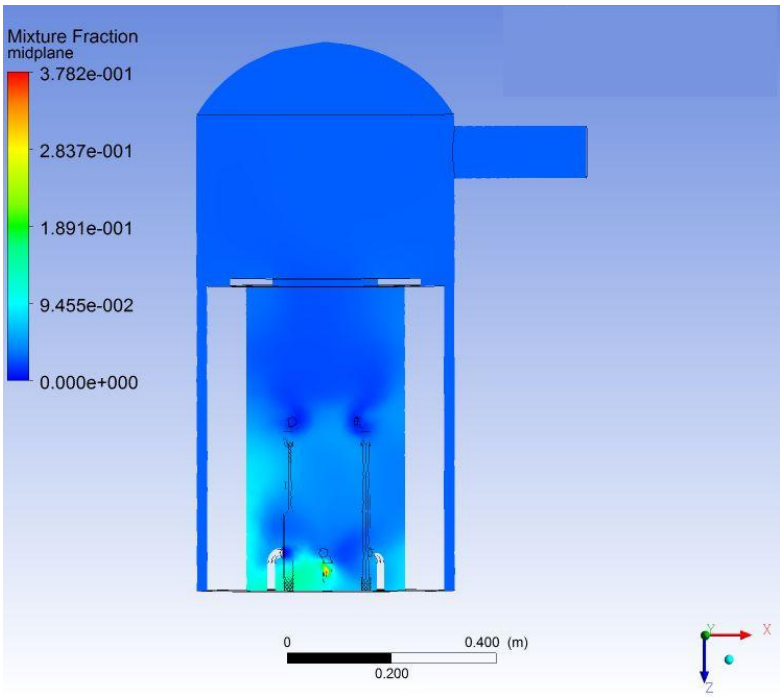


**Figure 6.3 : Fuel mass fraction contour**

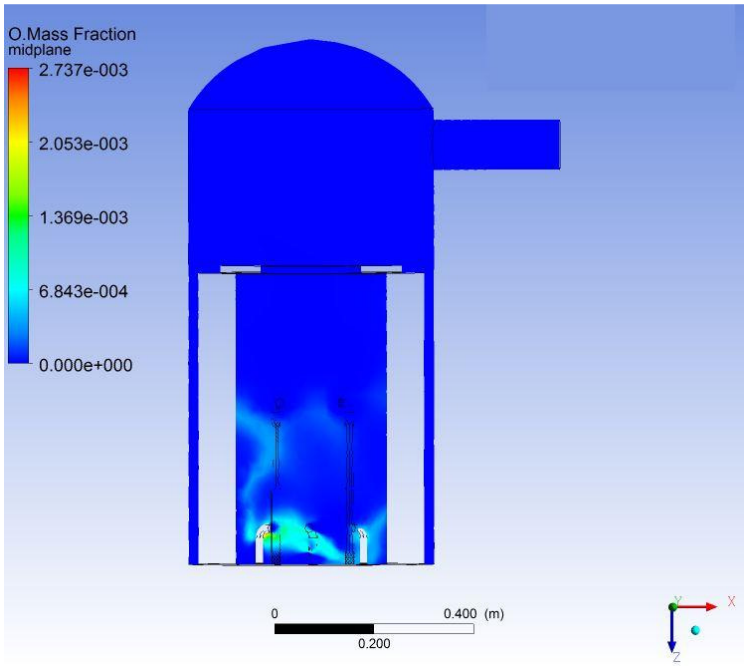


**Figure 6.4 : O radical mass fraction contour**

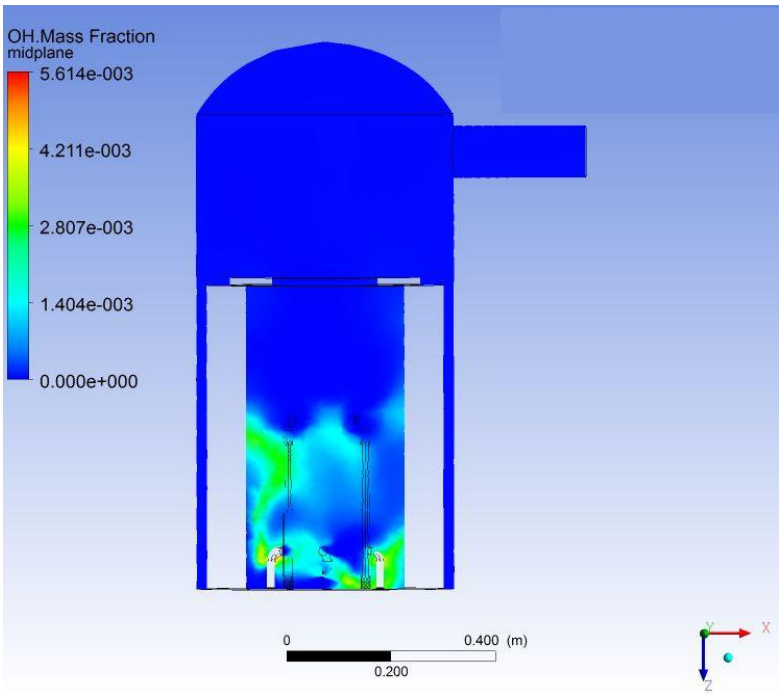


**Figure 6.5 : OH radical mass fraction contour**

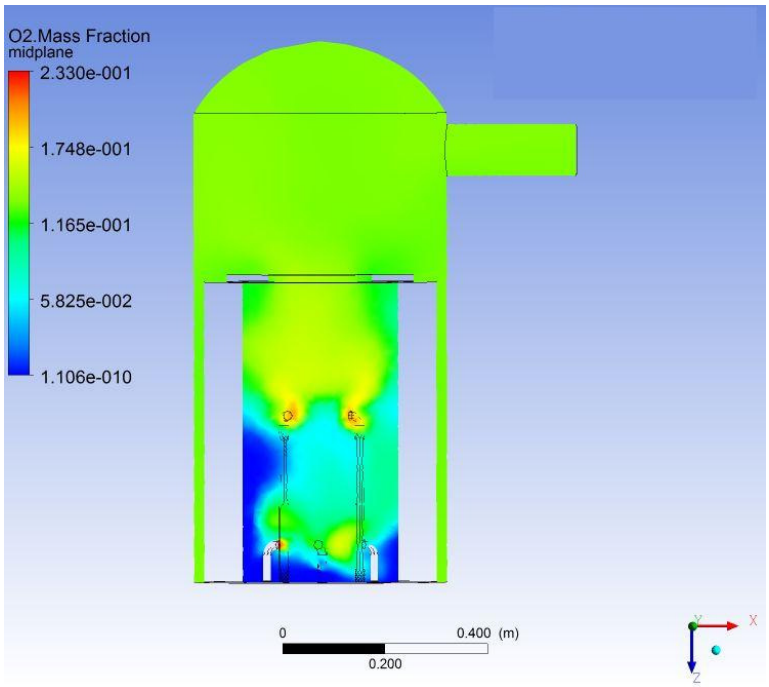


**Figure 6.6 : Oxygen mass fraction contour**

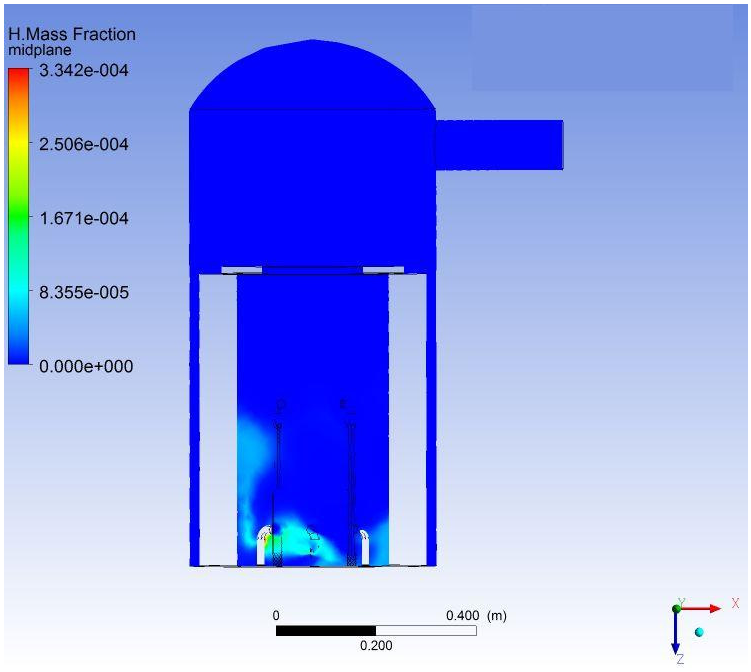


**Figure 6.7 : H radical mass fraction contour**

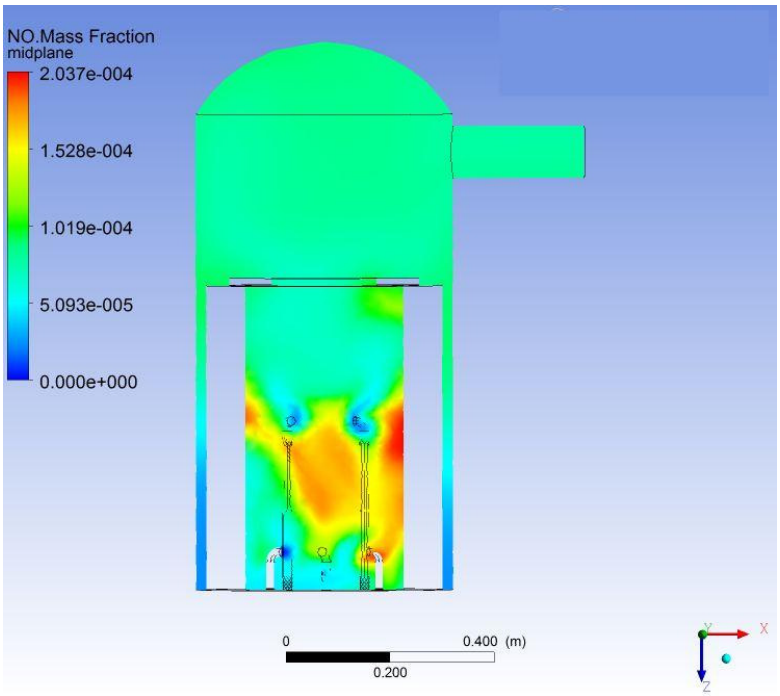


**Figure 6.8 : NO mass fraction contour**

From the temperature plot in figure 6.2 we can clearly see the effects of primary and secondary air streams. The fuel is injected at the center of the base of the combustor. Combustion occurs at higher local equivalence ratios resulting in relatively high temperatures. This forms the primary section. Then the dilution tubes downstream of the combustor add relatively cold secondary air and bring down the temperatures to the desired levels for the turbine. The O and OH radical mass fraction is an indicator of the flame region. It clearly shows that the flame is confined to the primary section of the combustion chamber.

### 6.2.2 Flamelet model and jet-A liquid spray multiphase simulations

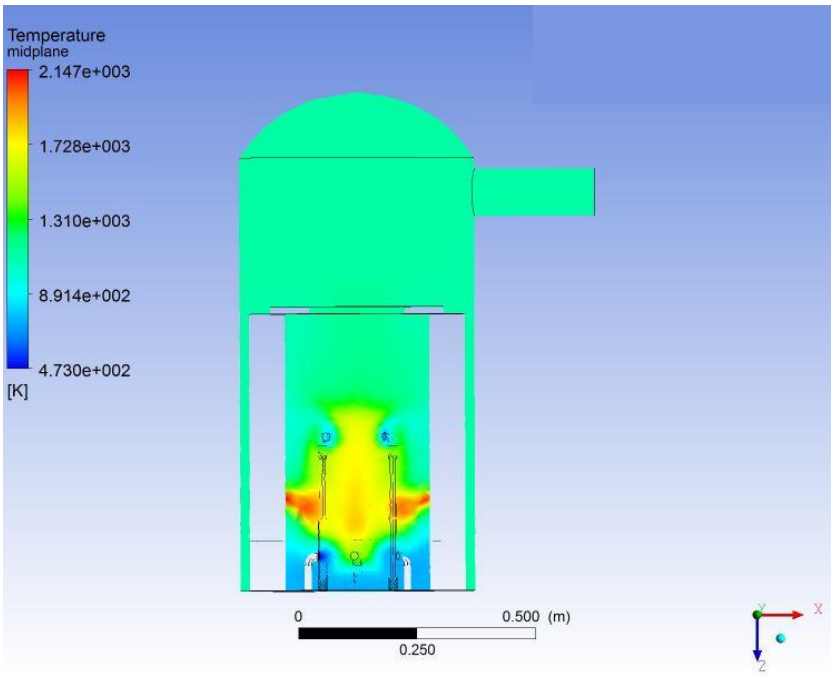


**Figure 6.9 : Temperature contour for liquid phase Jet-A spray**

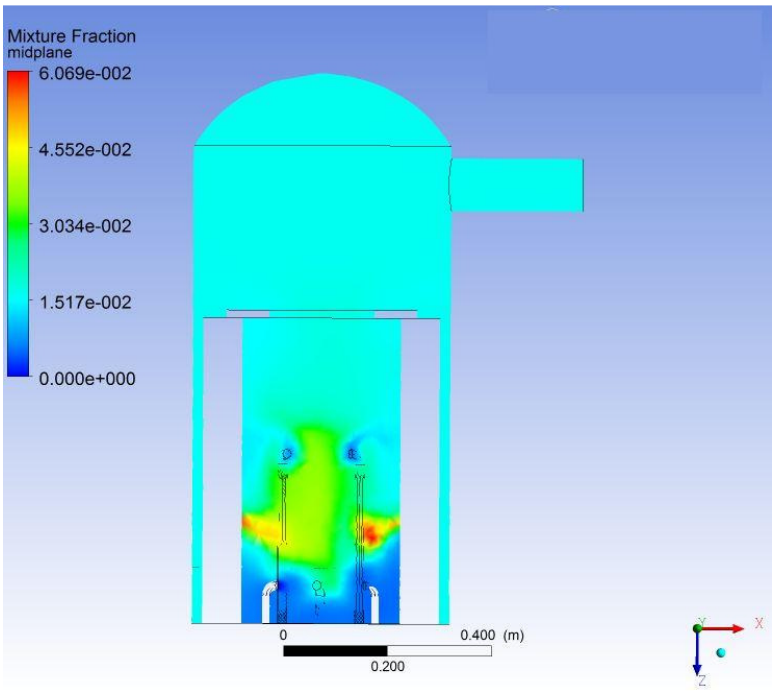


**Figure 6.10 : Fuel mass fraction contour**

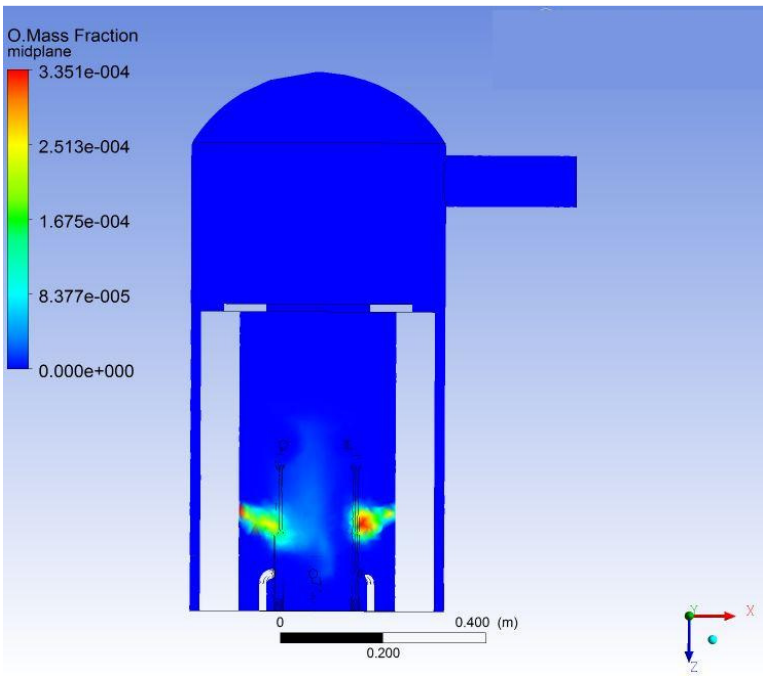


**Figure 6.11 : O radical mass fraction**

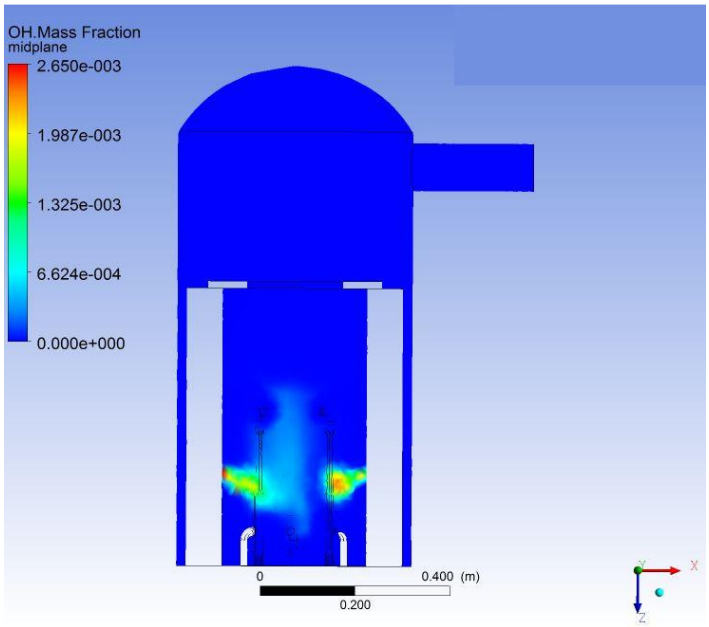


**Figure 6.12 : OH radical mass fraction**

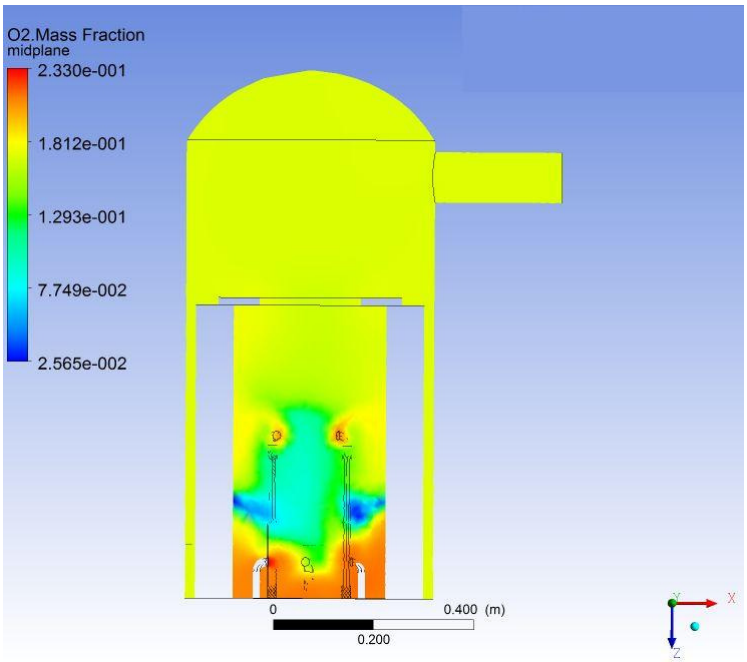


**Figure 6.13 : Oxygen mass fraction contour**

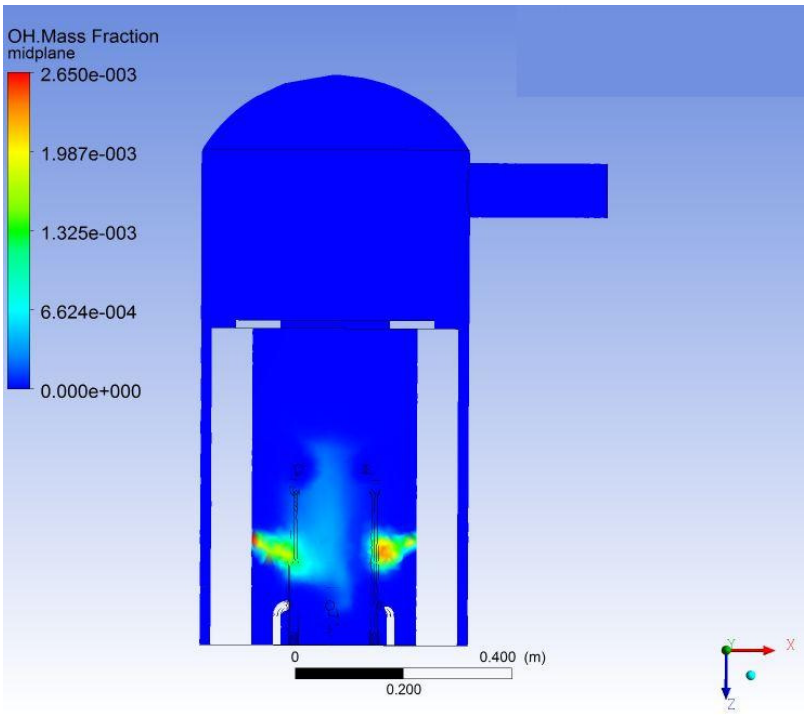


**Figure 6.14 : OH radical mass fraction**

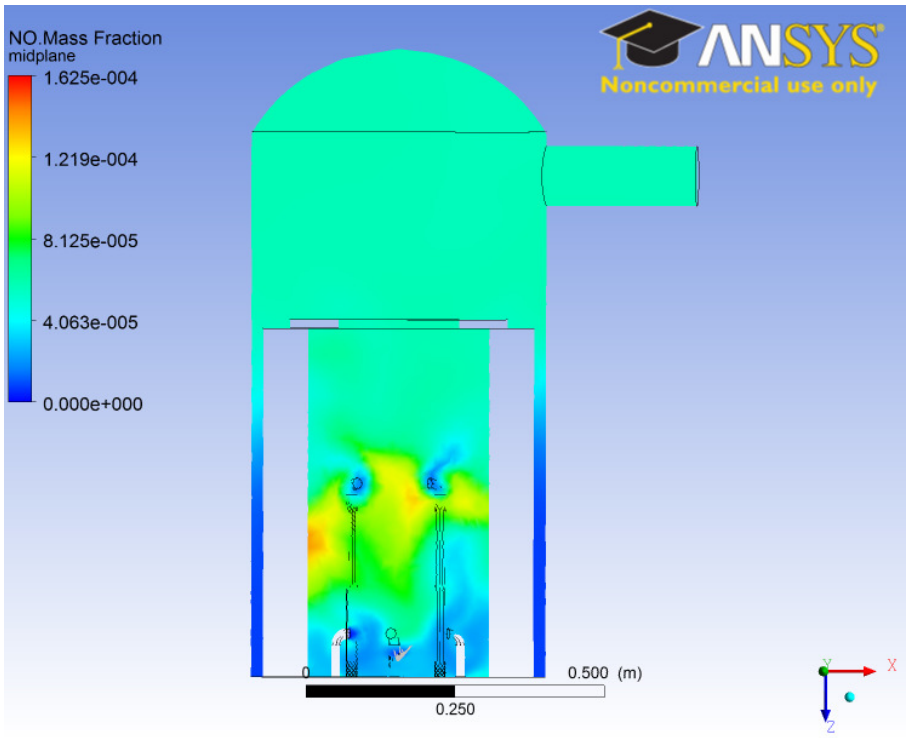


**Figure 6.15 : NO mass fraction contour**

From Fig. 6.3 and 6.2 we can clearly see the differences between the gas phase and multiphase simulation. The liquid spray is a hollow cone with a spray angle of 80°. We can see a lift off of the flame as compared to the gas phase simulations in Fig. 6.2. The experimental tests on this design also prove that we are able to burn Jet-A for an equivalence ratio of 0.4.

### 6.2.3 Flamelet model and glycerin evaporation model

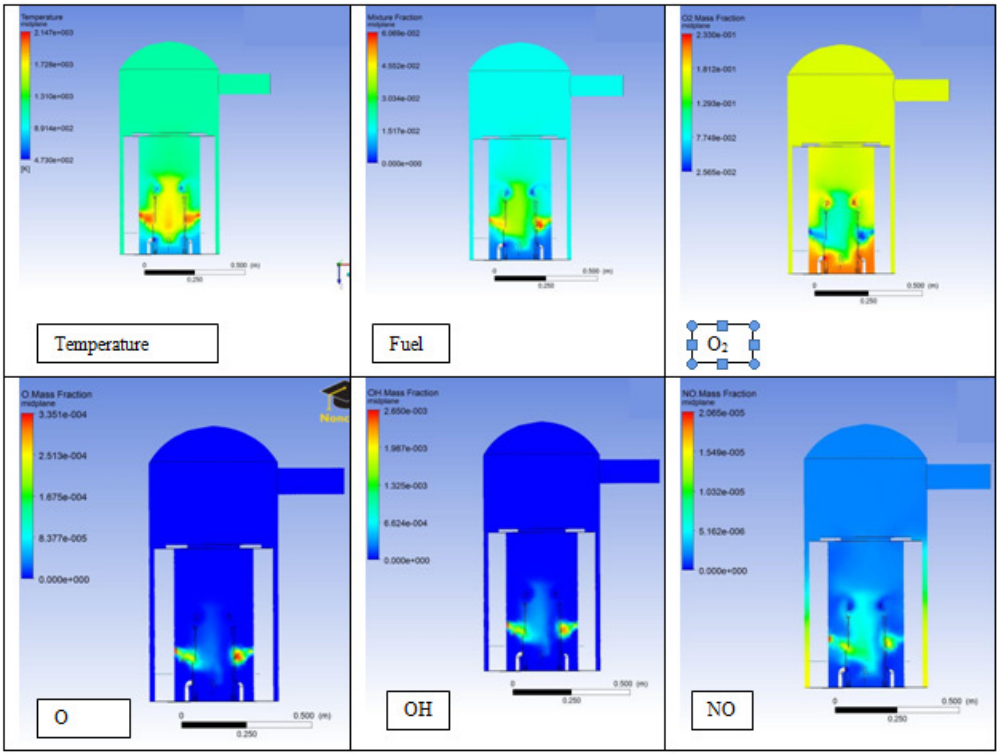


**Figure 6.16: CFD results for final design with glycerin evaporation rate.**

Finally the evaporation rate of liquid Jet-A was modified with the Anotine equation coefficients for glycerin. This would simulate the evaporation of glycerin. We observe from the temperature and fuel mass fraction contours that this design is suitable for burning glycerin as opposed to the first design in **Fig. 4.11.** The experimental trials on this design with glycerin as a fuel were successful. The system was first started with Jet-A. Then after preheating the system a switch over to glycerin was made and this design was able to burn glycerin successfully.

## 6.3 Emissions

Experimental measurements:

| | Units | Jet – A | Glycerin | 80/20 |
|---|---|---|---|---|
| N2 | % | 80.8 | 78.4 | 67.2 |
| O2 | % | 12.2 | 19.1 | 15.9 |
| CO2 | % | 7.3 | 4.3 | 3.4 |
| CO | % | 0.04 | 0.19 | 0 |
| NOx | ppm | 60 | 14.5 | 56 |
| UBHC | ppm | <50 | <150 | <65 |

CFD predictions for Jet-A: NOx - 57 PPM

$O_2$ - 13%

$CO_2$ - 7.9%

$N_2$ - 74.8%

The predictions from the CFD model match closely with the experimental results.

# Chapter 7

## Conclusions

In the above work we designed a gas turbine cyclone combustion chamber that can burn glycerin. The difficulty of its high viscosity was solved by pre heating the fuel. For a turbulent swirling diffusion flame, increasing the swirl number shortens the flame length. Highly swirling flows would be instrumental in burning viscous fuels in gas turbines. The swirl number is an important design parameter. Locating the recirculation zones is important and an effort should be made so that the fuel is sprayed in such a way that it flows into the recirculation zone and thus having maximum residence time. This would dictate the optimum spray angle for a given burner. CFD simulations show remarkable difference in temperature profiles and NOx emissions for different design configurations and liquid sprays. For the same global equivalence ratios the configurations which burn without the dilution tubes have lower NOx emissions as compared to those which burn rich and then quench the flame using the dilution air. However the earlier case cannot be used if we want to burn lean outside the flammability limit. For burning a fuel in gas turbines at very low equivalence ratios outside the flammability limits we should burn rich initially and then dilute the burnt mixture using dilution air. Thus we have to compromise between NOx emissions and flammability. Simulations also indicate that the NOx emissions would be the lowest for a premixed flame as in this case we do not have the high temperature regions where all the combustion occurs. Thermal NOx predictions from CFD matched closely with the experimental results. Even

though we did not have a kinetic model for glycerin combustion it was proved that owing to high Damkohler numbers, modeling the evaporation process of glycerin can give us a good approximation of our design. This was verified by the experimental results from the first design.

## References


1. IEA World Energy Outlook – 2010.

2. M.D. Bohon, B.A. Metzger, W.P. Linak, C.J. King, W.L. Roberts, Proceedings of the Combustion Institute 33 (2011) 2717-2724.

3. S. Anger, D. Trimis, B. Stelzner, Y. Makhynya, S. Peil, International Journal of Hydrogen Energy 36 (2011) 7877-7883.

4. D. Bombos, L. Mihaescu, I. Pisa, I. Bolma, G. Vasilievici, E. Zaharia, Revista de Chime 62 (2011) 562-566.

5. L. Wei, L.O. Pordesimo, A. Haryanto, J. Wooten, Bioresource Technology 102 (2011) 6266 6272.

6. JohnsonDT, TaconiKA. The glycerin glut: options for the value added conversion of crude glycerol resulting from biodiesel production. Environmental Progress 2007;26:338e48.

7. Beer,J.M., and Chigier, N.A., Combustion Aerodynamics, Applied Science Publishers, London,1972.

8. Drake, P.K., and Hubbard, E.F., J. Inst. Fuel 39,98(1966).

9. Kerr, N.M., and Fraser J.Inst.Fuel,38(1965),p.519.

10. M.L. Mather, N.R.L. Maccallum J.Inst. Fuel, 40(1967), p.214.

11. V.N. Afrosimova Thermal Eng., 14(1)(1967), p.10.

12. N. Syred, N.A. Chiger, J.M. Beer Poroc. 13$^{th}$ Int. Symposium on Combustion, The combustion Insitute, Pittsburgh, Pa.,(1971), p.563.

13. Combustion in swirling flows: A review, Combustion and Flame Vol.23,Issue 2(1974),Pages(143-201).

14. N.A.Chiger, A. Chervinsky, Trans.ASME J.Applied Mechanics, E34(1967), p.478.

15. Ross and Heideger, 1962 Ross, G.R.; Heideger, W.J., *Vapor pressure of glycerol*, J. Chem. Eng. Data, 1962, 7, 505-507.

16. Yaws' Handbook of Antoine Coefficients for Vapor Pressure (2nd Electronic Edition).

17. Lefebvre, A.H., 1999. Gas Turbine Combustion, Taylor and Francis.

18. CFX help manual.